GLCTTR 27/91-1

Investigaton of the Performance of a Headway Control system for Commercial Vehicles

Z. Bareket
The University of Michigan
Transportation Research Institute
Ann Arbor, Michigan 48109

P. Fancher
The University of Michigan
Transportation Research Institute
Ann Arbor, Michigan 48109

G. Johnson
The University of Michigan
Transportation Research Institute
Ann Arbor, Michigan 48109

January, 1993

Great Lakes Center for Truck Transportation Research

University of Michigan Transportation Research Institute, 2901 Baxter Road, Ann Arbor, MI 48109-2150

DISCLAIMER

The contents of this report reflect the views of the authors, who are responsible for the facts and the accuracy of the information presented herein. This document is disseminated under the sponsorship of the Department of Transportation, University Transportation Centers Program, in the interest of information exchange. The U. S. Government assumes no liability for the contents or use thereof.

ACKNOWLEDGEMENTS

The authors wish to acknowledge the support for this work by the U. S. Department of Transportation, through a grant to the Great Lakes Center for Truck Transportation Research.

This report was originally published as:

Baraket Z, Fancher P S, and Johnson G. "Investigaton of the Performance of a Headway Control System for Commercial Vehicles." The University of Michigan Department of Transportation Research Institute, Report No. UMTRI-93-2 and IVHS Tech. Rept. 93-01, 1991, 41 p.

Technical Report Documentation Page

1. Report No.	2. Government Accession No.	3. Recipient's Catalog No.
GLCTRR-27/91		

4. Title and Subtitle	5. Report Date
Investigation of the performance of a headway control system for commercial vehicles	January, 1993
	6. Performing Organization Code
7. Author(s)	8. Performing Organization Report No.
Z. Bareket, P. Fancher, G. Johnson	UMTRI-93-2 IVHS Tech. Rept. 93-01
9. Performing Organization Name and Address	10. Work Unit No. (TRAIS)
The Universityof Michigan Transportation Research Institute 2901 Baxter Road, Ann Arbor, MI 48109	11. Contract or Grant No.
	13. Type of Report and Period Covered
12. Sponsoring Agency Name and Address Great Lakes Center for Truck Transportation Research and University of Michigan IVHS Industrial Affiliates Program 2901 Baxter Road Ann Arbor, Michigan 48109	14. Sponsoring Agency Code

15. Supplementary Notes

Supported by a grant from the U.S. Department of Transportation, University Transportation Centers Program

16. Abstract

A concept for implementing headway for commercial vehicles is introduced. Developing a headway system is motivated by the desire to improve safety and enhance mobility through the use of longitudinal control. Such control is carried out via two possible modes of operation: cruise control mode and headway control mode. The headway-control system consists of range and range-rate sensors, a cruise control capable of accepting velocity commands and a control unit using a heuristic algorithm for determining the appropriate mode of operation and for selecting that mode. When in a headway control mode, the system utilizes information from the range and range-rate sensors to maintain a prescribed headway from a leading vehicle. When in a cruise control mode, the system maintains the speed selected by the driver. The equations of motion that mathematically represent the vehicle are derived, and a system model for simulation is constructed. An analysis by simulation is performed to demonstrate that reasonable performance of the system can be expected. The following desired step in this investigation is to install the system in a heavy truck, and to conduct experiments to verify that the system performs as predicted or, at least, that the system can be made to perform satisfactorily.

17. Key Words	18. Distribution Statement
Intelligent Vehicle Highway Systems, Headway Range, Range Rate, Cruise, Sensors	

19. Security Classif. (of this report)	20. Security Classif. (of this page)	21. No. of Pages	22. Price
		41	

Investigation of the Performance of a Headway Control System for Commercial Vehicles

Z. Bareket

P. Fancher

G. Johnson

Abstract

A concept for implementing headway control for commercial vehicles is introduced. Developing a headway control system is motivated by the desire to improve safety and enhance mobility through the use of longitudinal control. Such control is carried out via two possible modes of operation: cruise control mode, and headway control mode. The headway control system consists of range and range rate sensors, a cruise control capable of accepting velocity commands, and a control unit using a heuristic algorithm for determining which is the appropriate mode of operation, and for selecting that mode. When in a headway control mode, the system utilizes information from the range and range rate sensors to maintain a prescribed headway from a leading vehicle. When in a cruise control mode, the system maintains the speed selected by the driver. The equations of motion that mathematically represent the vehicle are derived, and a system model for simulation is constructed. An analysis by simulation is performed to demonstrate that reasonable performance of the system can be expected. The following desired step in this investigation is to install the system in a heavy truck, and to conduct experiments to verify that the system performs as predicted or, at least, that the system can be made to perform satisfactorily.

Keywords

Intelligent Vehicle Highway Systems, Headway, Range, Range rate, Cruise, Sensors

Table of Contents

NOMENCLATURE

Symbol	Definition
A	Frontal area, (ft^2)
C_d	Air drag coefficient
C_r	Rolling resistance coefficient
C_s	Longitudinal stiffness, tire, (lb)
C.R.	Compression ratio
F_{aero}	Resisting force, aerodynamic, (lb)
F_{roll}	Rolling resistance, tire - total, (lb)
F_t	Drive force, tire - total, (lb)
F_x	Longitudinal force, tire, (lb)
F_θ	Resisting force, grade, (lb)
HP	Gross engine power, (horsepower)
I_d	Rotational inertia, drivetrain, ($ft\text{-}lb\text{-}sec^2$)
I_e	Rotational inertia, engine, ($ft\text{-}lb\text{-}sec^2$)
I_{ax}	Rear axle ratio
I_g	Transmission gear ratio
K_i	Cruise-control integration gain
K_p	Cruise-control proportioning gain
m	Mass of vehicle (lbm)
$P_{emp_{loss}}$	Motoring losses, mean effective pressure, engine, (psi)
P_r	Atmospheric pressure, (in-Hg)
R	Range, leading to trailing vehicle, (ft)
$\dot{R}$	Range rate, (mph)
R_d	Disengage range, (ft)
R_s	Constant range-switching distance, (ft)

R_t	Rolling radius, tire, (ft)
s	Slip, tire
S	Piston stroke, (in)
T_d	Headway time, (sec)
T_e	Momentary engine torque, (lb-ft)
$T_{friction}$	Friction torque losses, engine, (lb-ft)
T_{gross}	Gross engine torque, (lb-ft)
T_{loss}	Engine torque losses, (lb-ft)
T_r	Ambient temperature, ($^{\circ}R$)
T_s	Switching time, (sec)
T_t , $T_{traction}$	Engine torque generating traction, (lb-ft)
V	Speed, (fps)
V_1	Speed, 'trailing' vehicle, (mph)
V_2	Speed, 'leading' vehicle, (mph)
V_c , $V_{control}$	Control speed, (mph)
V_d	Cruise speed, driver selected, (mph)
V_H	Engine displacement, (in^3)
$\mathcal{V}_p$	Mean piston speed, (fpm)
W	Weight of vehicle (lb)
δ_t	Throttle position
ε	Speed error at cruise control, (mph)
η_d	Mechanical efficiency, drivetrain
η_v	Volumetric efficiency, engine
θ	Road grade, (rad)
ρ	Air density, ($lb\text{-}sec^2/ft^4$)
ω, ω_e	Engine speed, (rpm)
$\overline{\omega}_t$	Rotational speed, tire (rps)

Investigation of the Performance of a Headway Control System for Commercial Vehicles

Z. Bareket

P. Fancher

G. Johnson

1.0 INTRODUCTION

The objective of this project is to develop a basic understanding of the concepts involved with a headway-control system. Investigating the components, control strategies, and human interface issues of such a system will facilitate the identification of research needs within this application.

The addition of control systems to highway vehicles has received much attention in recent years. The current interest in improving safety and enhancing mobility through the use of longitudinal and lateral control systems is being actively pursued throughout the world in programs such as PROMETHEUS, IVHS, SSVS, etc. Much of this work pertains to the development of control systems for passenger cars.

Noting that the power-to-weight ratios of heavy trucks make them quite different from passenger cars with regard to maintaining speed and headway, a research project was undertaken here to address the truck-specific issues in longitudinal control. This research investigation focuses on the performance of a vehicle system consisting of a heavy truck, range and range-rate sensors for following the motion of a leading vehicle, a cruise control modified to accept velocity commands, and a control unit using a heuristic algorithm for switching in and out of a headway-control mode.

The equations of motion, employed in an analysis by simulation, include engine and drive system properties plus longitudinal dynamics and tire force characteristics. The cruise control has proportional and integral control to compensate for speed errors due to disturbances such as upgrades or downgrades. The headway-control unit has a number of nonlinearities requiring compensation, including full accelerator saturation, which prevails when the heavy truck may be operating at full throttle for extended periods of time. The analysis includes the development of switching rules that depend upon conditions such as insufficient time remaining before impact, and insufficient headway distance remaining. The desired level of headway and time to impact may also be set by the driver or

established through simulation experiments as fixed parameters of the system. At this initial stage, the analysis is oriented toward physical interpretations of the results, noting that the control algorithms have been based only upon preliminary judgments of the predicted performance of the system.

Since the analysis shows that reasonable performance of the system can be expected, attempts are being made to mock up a system using (a) existing equipment for measuring range and range-rate and (b) a prototype control unit that has been calibrated based upon results from the simulation. Experiments will be conducted to establish system performance properties, and the simulation model will be refined so as to predict actual performance. The results will be used in defining an experimental capability for evaluating headway control systems and for performing studies of driver preferences and characteristics when using a headway control system.

This report describes the concept developed for extending a cruise control functionality to a headway control system, the model used for simulating the performance of the resulting system, and the simulation results that illustrate how the system would perform in a heavy truck.

2.0 CONCEPT NARRATION

Systems that are aimed at automatically controlling the speed of a motor vehicle can be classified into two main categories: independent systems, and those whose proper function depends on external inputs. The first type is commonly known as *cruise control.* The concept of such a system is that the driver sets the desired speed, and, as long as the system is engaged, the throttle is controlled to maintain that speed, independent of external factors. The second type, commonly called intelligent, or "smart," cruise control, automatically controls the headway between the equipped vehicle and the vehicle ahead, whenever the preset cruise speed causes one vehicle to overtake another. No action is required from the driver of the headway-adaptive system under these circumstances. In the case of interferences for which the system cannot adapt, the system disengages itself and issues a warning to the driver to resume direct control of the throttle.

The general layout that describes the conventional cruise-control function is portrayed in figure 1. The system utilizes a single control input, which is the speed at which the vehicle will cruise, selected by the driver. By monitoring the error signal between the desired speed and the actual speed of the vehicle, the cruise-control system compensates

and changes the throttle setting to achieve a zero error signal. One major disadvantage of such a system is illustrated by the situation when, ahead of the "cruising" vehicle, on the same lane, a slower vehicle is encountered. As it approaches the slower vehicle from behind, the driver of the faster vehicle must either disengage the cruise control or change lanes to avoid the imminent rear-end collision. This situation, commonly encountered when using a cruise-control system, has safety implications; the driver must anticipate traffic interference and take timely action to override the cruise control. It also affects operational fuel economy as the engine fuel supply is being switched back and forth from automatic to manual control.

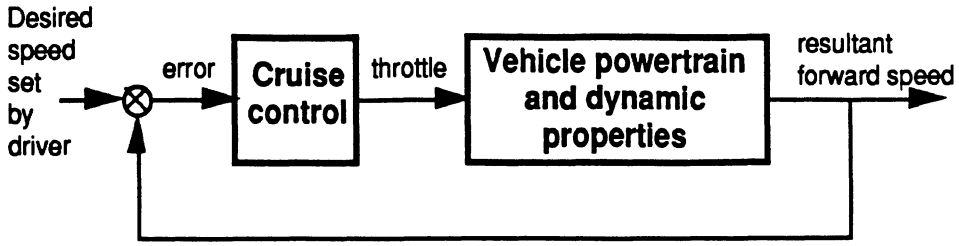

Figure 1. Cruise control

The intelligent cruise control function is illustrated in figure 2. A distance-measuring sensor installed at the front of the vehicle picks up the range from the vehicle ahead. The rate of change in the range variable is also acquired. The headway-control unit continuously accepts the range, range rate, present vehicle speed, and driver's desired speed selection. The *headway mode* of operation prevails whenever the control system modulates throttle so as to maintain a constant range from the lead vehicle (whereupon the controlling speed value is that of the leading vehicle). The *cruise mode* of operation prevails when the system functions as a conventional cruise control (whereupon the controlling speed value is that which has been set by the driver). The system uses a heuristic algorithm to switch between the headway and cruise-control modes, or to disengage itself altogether and activate a warning signal if a rear-end collision is imminent.

At least in concept, the intelligent cruise-control system may also function to avoid collisions with stationary obstructing objects (parked vehicles or other obstacles). By continuously evaluating the gap (and its rate of change) between the vehicle and the object ahead (a slower vehicle or any other obstacle), the unit can assess the situation and take appropriate action.

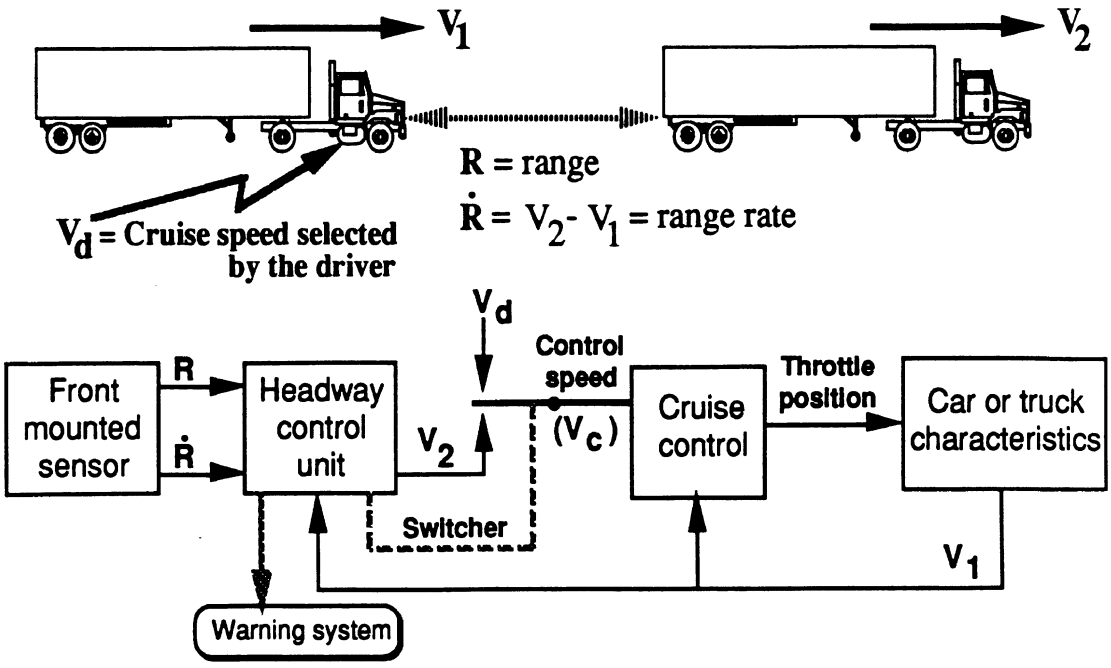

Figure 2. Headway control

3.0 SYSTEM MODEL CONSTRUCTION

The notion of headway control as presented in this work with its various concepts and elements is being evaluated for applications to cars, trucks, and busses. Nevertheless, power-to-weight ratios and inertial characteristics of heavy trucks make them unique and distinct from passenger cars and other lighter vehicles with regard to accelerating and maintaining speed. The system model constructed here is aimed at evaluating performance of headway control systems installed in heavy trucks.

Simulating the operation of the headway control system requires a mathematical model of the following components from figure 2:

- Headway-control heuristic algorithm (speed and headway-control modes switching)
- Cruise control (throttle position control for speed maintenance)
- Vehicle propelling characteristics (forward speed response for driver's input)

This section describes the different methods used to form the various models required to generate the headway-control system simulation.

3.1 Headway control

The headway-control unit requires three inputs for its proper operation: (1) range from the lead vehicle (or from the obstacle ahead), R; (2) rate of change of that range, $\dot{R}$; and (3) present speed of the vehicle, V_1. The fundamental concept of the heuristic algorithm used by this control system is headway "cushioning." If the combination of the range and its rate of change is within certain boundaries, the system tracks the speed of the lead vehicle. During tracking, the headway gap is adjusted to provide adequate cushioning for upcoming speed and distance adjustments that may become necessary. If the combination of range and range rate indicates the possibility of an imminent rear-end collision, the system disengages itself and activates an appropriate warning (automatic brake application can also be considered). When the system's interpretation of the range and range rate indicates that the lead vehicle either accelerated or departed the lane so that it is no longer an obstruction, the system returns to normal cruise-control operation, and accelerates to the speed set by the driver.

Figure 3 portrays the heuristic algorithm of the headway-control system. The operational modes are defined by the various boundary lines shown in the figure. These lines are described below. Four parameters are adjustable at the user level to facilitate a safety "comfort zone," or to implement fleet operational policies if applicable:

R_d Disengage range. This parameter is the minimum range value with which the driver is "comfortable," for automatic headway control by the system — regardless of the gap trend. When the range from the lead vehicle becomes shorter than R_d, regardless of its derivative, the system must activate a warning and disengage itself.

R_S Constant range switching distance. This parameter defines the maximum value of intervehicle range within which the system will seek to maintain headway. Under steady-state conditions ($\dot{R} = 0$), if the range is larger than R_S, the system will accelerate the vehicle (up to the preset speed value, V_d) to close the gap. Usually the R_S value is determined based on the traffic load. Setting R_S too large will encourage other vehicles to "squeeze" into the gap, while setting it too small will not allow for headway cushioning.

T_d Headway time. Large fleets (e.g. *Greyhound*) may have a policy that refers to this parameter in term of "X seconds of safety distance". In practice, this is the time that elapses between the passage of two successive vehicles by a fixed point

on the road. As shown in figure 3, T_d constitutes the slope of the *disengage* line. Any combination of range and range rate located below this line will result in a warning and the subsequent transfer of control to the driver.

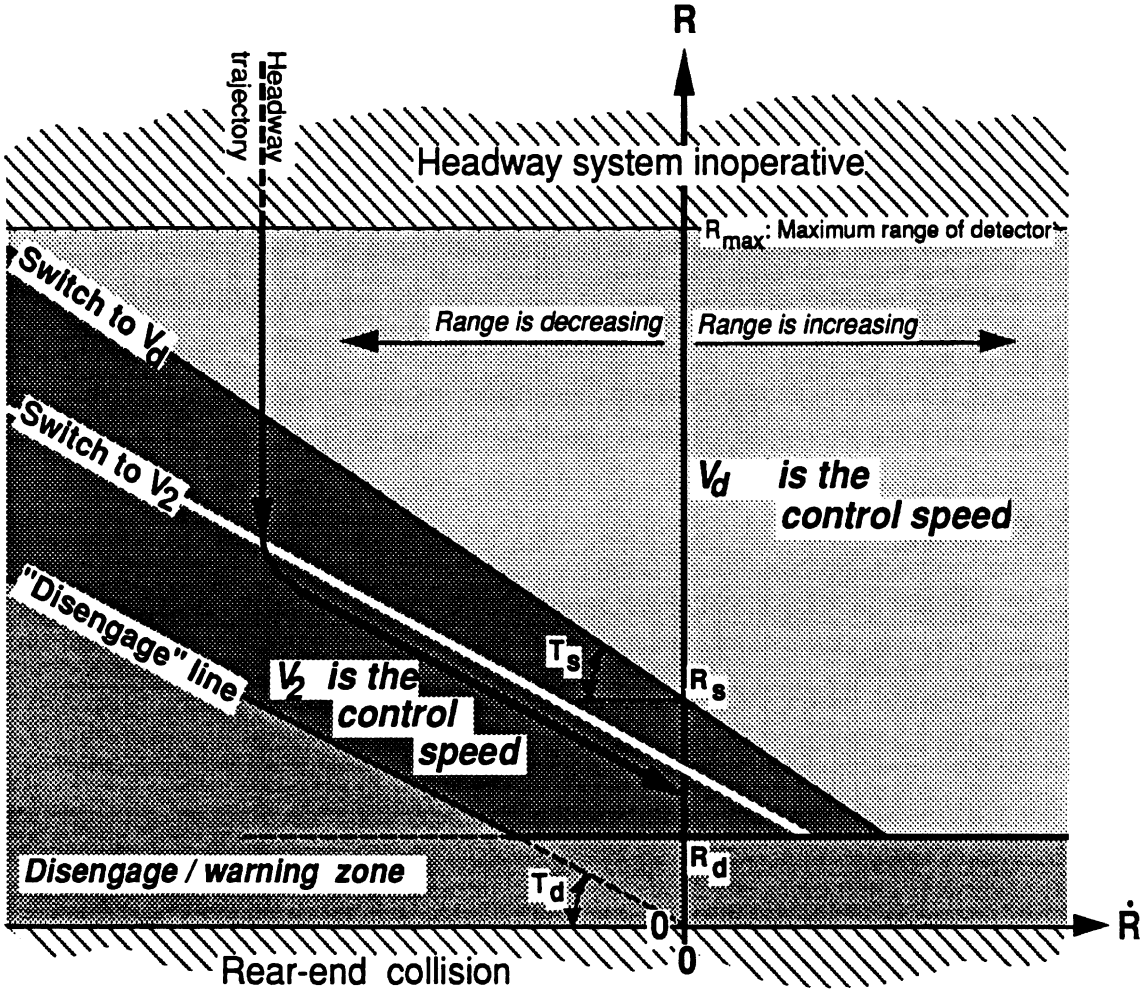

Figure 3. Headway control algorithm

T_S Switching time. This parameter represents the slope of the boundary line between the respective zones of cruise-control mode and headway mode. In general, range and range-rate combinations that are located above this line define the zone of cruise-control mode, and those below the line (but above the disengage line) define the zone of headway mode. Following the headway trajectory in figure 3, no change in operation mode takes place when the "Switch to V_d" line is crossed. The system changes to the headway mode only after the "Switch to V_2" line is crossed. The line "Switch to V_d" will affect the operational mode of the system only if the headway trajectory crosses it again from below. In that case, V_d will

become the control speed (cruise-control mode). To summarize this switching condition, the system switches to headway-control mode when "Switch to V_2" is crossed from above, and switches to cruise-control mode when "Switch to V_d" is crossed from below. This feature allows for headway cushioning, and it is introduced to avoid control fluctuations that tend to appear if the operation mode is determined only by the "Switch to V_d" line. Practically, the value of T_s is set to be close to T_d — it can be either equal to it or larger, but not smaller. Setting $T_s < T_d$ will result in convergence of the two lines, so that in cases of high rates of range closing, even with more than adequate spacing, the system might disengage without entering the headway mode.

Important relationships that pertain to figure 3 and the headway control algorithm are given below:

$$V_2 = \dot{R} + V_1 \tag{1}$$

$$R_{switching} = R_s - T_s \cdot \dot{R} \qquad \text{(Switching line equation)} \tag{2}$$

$$R_{disengage} = -T_d \cdot \dot{R} \qquad \text{(Disengage line equation)} \tag{3}$$

A typical operational scenario of the headway-control system is depicted by the headway trajectory line in figure 3 (see also the Simulation Results" section of the report). The driver of vehicle one (V_1 in figure 2) sets the cruise control to maintain a speed of V_d. Far ahead, on the same lane but beyond the reception limits of the range sensor, vehicle two cruises at speed V_2, which is slower than V_d (this situation pertains to the dotted part of the line). As the range goes below R_{max}, the system detects vehicle two (V_2) and starts monitoring the range between the vehicles and its rate of change (solid vertical line). Using equation (1), it also computes V_2. For illustration purposes, it is assumed that both vehicles maintain constant speeds at this point, so that $\dot{R}$ is unchanged. If this was not the case, the dashed and solid line coming from the top of figure 3 would have had a slope instead of being vertical. As vehicle one approaches vehicle two from behind, the switching line is crossed ($R < R_s - T_s \cdot \dot{R}$), but the cruising speed of V_d is still maintained until the "Switch to V_2" line is also crossed. This line is computed automatically by the headway system based on the parameters it was provided with, viz.:

$$R_{homing} = \frac{R_s + R_d}{2} - \frac{T_s + T_d}{2} \cdot \dot{R} \qquad \text{("Switch to } V_2\text{" line equation)} \tag{4}$$

When the "Switch to V_2" line is crossed, the system changes to headway mode, and the controlling speed is V_2. This line is tracked until the range between the vehicles is maintained constant with $\dot{R} = 0$.

3.2 Cruise control

The goal of a cruise-control system is to maintain a constant vehicle speed over a wide range of road conditions by changing throttle position as required. A well designed cruise-control system is noted by its ability to perform that task with smooth, yet minimal throttle movements. The basic control method of such a system is portrayed in figure 1, and a typical installation layout is illustrated in figure 4 (this particular example pertains to a diesel engine).

With the system on, the driver depresses the button to set the desired cruise speed. The control unit then combines that information and the current speed of the vehicle to determine the necessary throttle compensation. The resulting correction signal is then facilitated via the control valve to regulate the air pressure into the throttle actuator, which in turn moves the control lever of the fuel pump to accelerate or decelerate the vehicle. When either the brake or the clutch pedal is depressed, the air signal to the actuator is cut off to avoid engine overspeed.

A great deal of effort has gone into the design of cruise-control systems. The algorithms by which throttle adjustments are determined vary with the different systems [1]. Proportioning and integrating (PI) control algorithms employ proportioning and integration of the error signal to determine throttle adjustment, where proportioning and derivative (PD) methods augment proportioning with first and sometimes second order derivatives of the error signal. The PID cruise-control system is a combination of the PI and the PD algorithms: it uses proportioning, integration, and derivatives. In these systems, the gains used in the computations are constant. Each of these methods has both advantages and disadvantages, but common to them all is the fact that extreme variations in the operational conditions will result in performance levels that are inadequate to the point that the system needs to be adjusted to the new conditions. Newly designed, more sophisticated cruise-control systems that are mostly still under development utilize advanced control approaches such as *sliding control*, and *fuzzy logic* [1]. These methods are also referred to as *adaptive cruise control* systems [2, 3]. They are distinguished from the PI, PD, and the PID systems by their ability to self-adjust as changes in both

operational conditions and vehicle performance take place. Since the concept of the headway-control system entails an existing cruise-control system, no effort is made here to develop new approaches in cruise-control design. Nevertheless, for the purpose of simulating the function of a headway-control system, a mathematical model of a cruise control had to be derived.

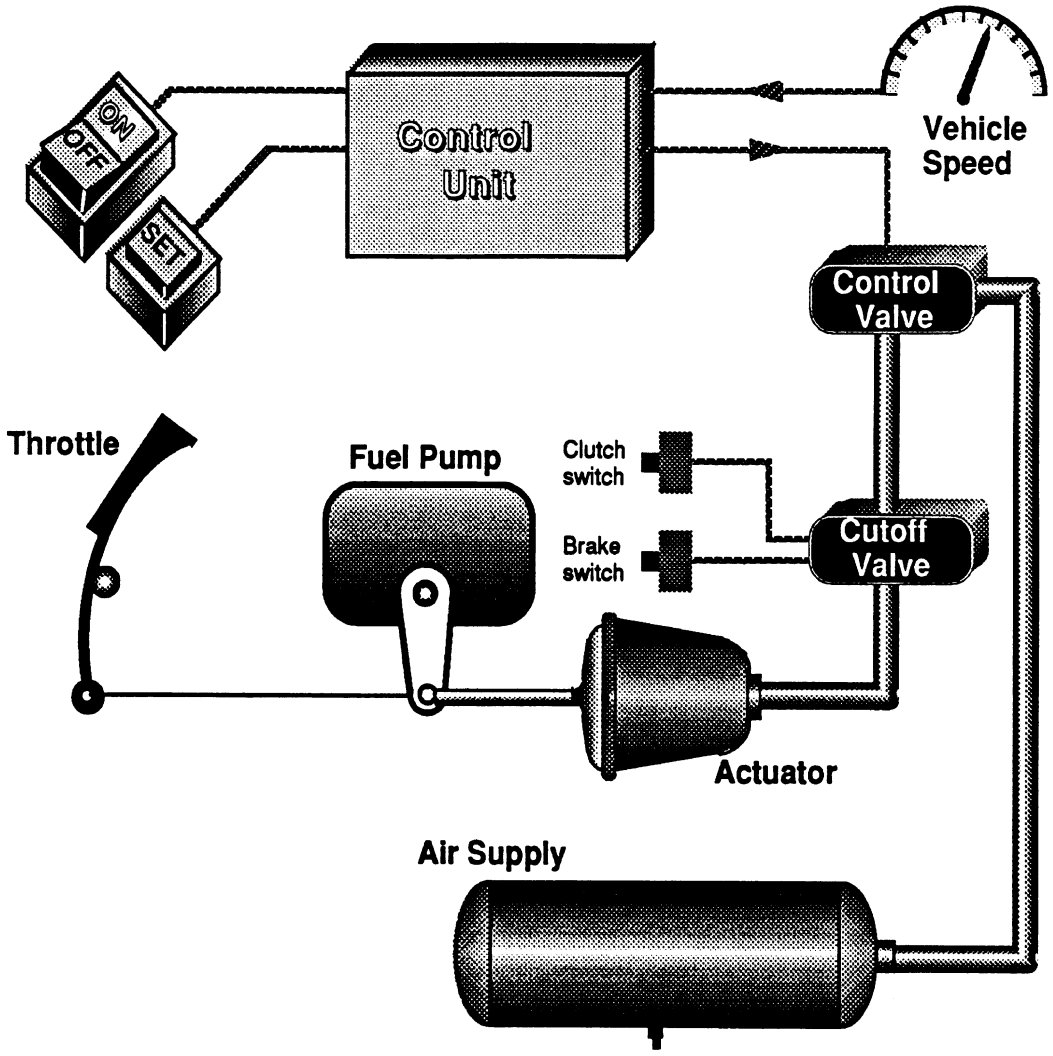

Figure 4. Cruise control — typical installation

The algorithm used to simulate the cruise control in this work is of the PI method [1, 4], which utilizes proportional and integral control. A block diagram representation of the system is given in figure 5. The error input to the cruise-control model is the speed difference by equation (5), where the controlling speed ($V_{control}$) is either the cruising

speed set by the driver (V_d) or the speed of the leading vehicle (V_2), according to the heuristic algorithm of the headway-control system described in the previous section. The throttle compensation output signal of the cruise control is given by equation (6).

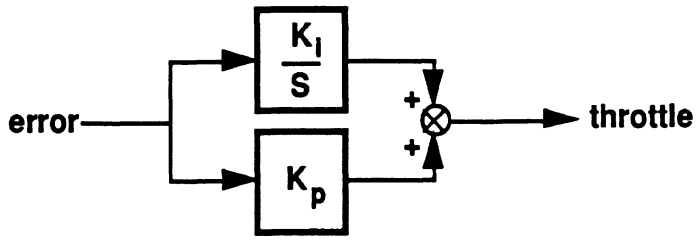

Figure 5. PI Cruise control

$$\mathcal{E} = V_{control} - V_1 \tag{5}$$

$$\delta_t = K_p \cdot \mathcal{E} + K_i \int \mathcal{E} dt \tag{6}$$

where:

$\mathcal{E}$	is the speed error input to the cruise control.
$V_{control}$	is the controlling speed as determined by the headway control system.
V_1	is the current truck speed.
δ_t	is the corrective throttle input.
K_p	is the proportioning gain of the system.
K_i	is the integration gain of the system.

3.3 Vehicle model

The model of the vehicle used in the simulation incorporates drive train properties and dynamics, tire-force characteristics, and a simplified mathematical representation of the engine. In the literature, several studies conducted in the past for spark ignition (SI) engines indicated simple, yet reliable ways to model such engines [5, 6]. Conversely, studies of diesel engines took very detailed steps into investigating the burning process, flame propagation, induction dynamics, and the motion of the various engine parts. For the purpose of simulating and assessing the concept of this headway control system, even the simpler of these models was considered too elaborate to be used [7]. Instead, simplifying assumptions were made, and a mathematical model for the simulation of a diesel engine was derived.

A block diagram representation of the engine and the vehicle model used in the simulation is given in figure 6. The analysis includes equations of motion that represent the following dynamic characteristics and features of the vehicle:

- Longitudinal forces acting on the vehicle (aerodynamic, grade, traction)
- Longitudinal tire force characteristics (slip, stiffness)
- Rolling resistance of the tires
- Engine torque equation (based on speed and throttle setting)
- Torque generation lag
- Engine torque losses (internal friction, accessories)
- Rotational inertias of the powertrain (engine, transmission)

Longitudinal forces

The longitudinal motion of the vehicle is governed by the differential equation (7). The various forces it incorporates are discussed below. The acceleration of the vehicle ($\dot{V}$) is determined by the net force available, after the resisting forces are subtracted from the tractive force developed by the tires.

$$\mathbf{m} \cdot \dot{\mathbf{V}} = \mathbf{F_t} - \mathbf{F_\theta} - \mathbf{F_{aero}} - \mathbf{F_{roll}} \tag{7}$$

where:

m	is the mass of the vehicle (lbm.)
$\dot{V}$	is the longitudinal acceleration of the vehicle
F_t	is the total traction force of the tires
F_θ	is the resisting force due to grade
F_{aero}	is the aerodynamic resisting force
F_{roll}	is rolling resistance force of the tires

The traction force of the tires and the rolling resistance are described hereafter under the appropriate headings. Grade resisting force is given by equation (8), and is the weight component pulling down any body positioned on a slope.

$$\mathbf{F_\theta} = \mathbf{W} \cdot \mathbf{Sin}(\theta) \tag{8}$$

where:

θ	is the angle of the slope (radians)
W	is the weight of the vehicle (lbf.)

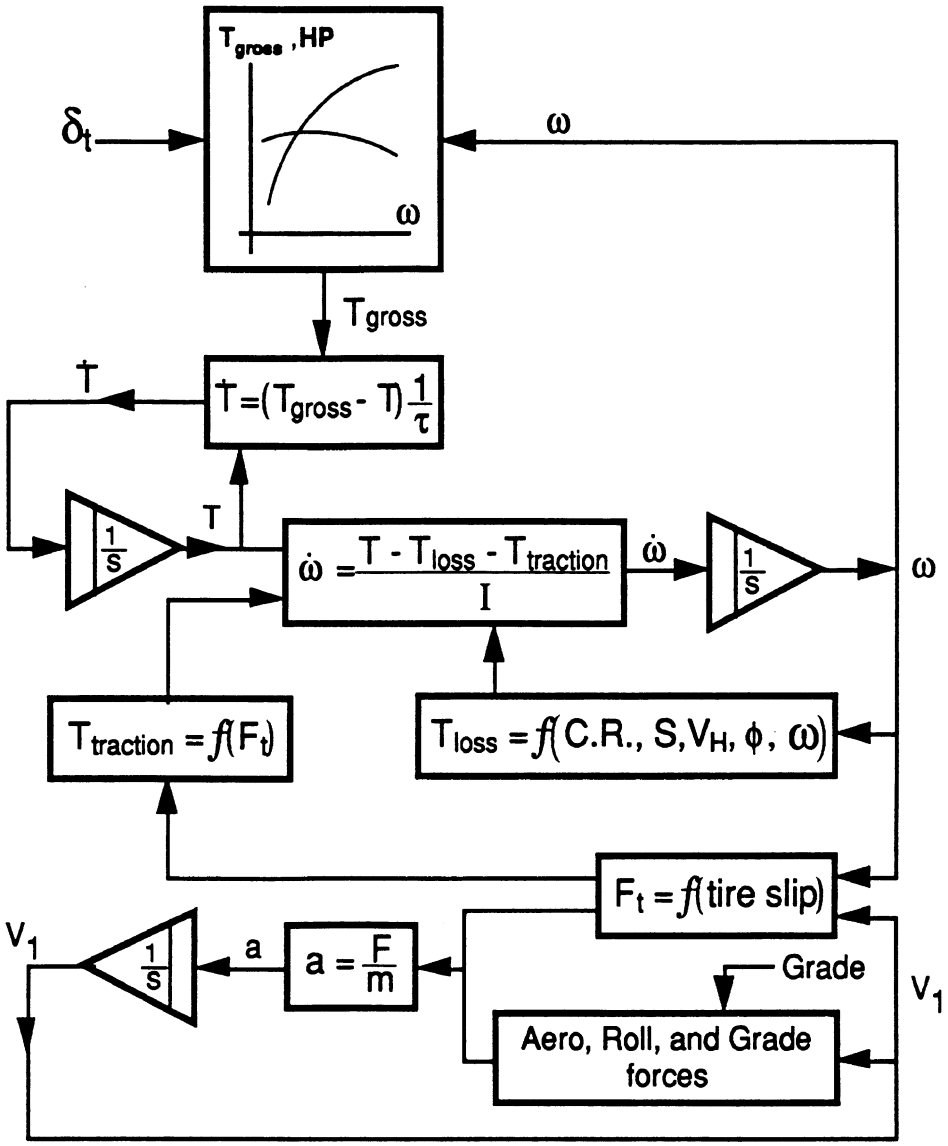

Figure 6. Engine and vehicle dynamic model

Aerodynamic forces act on a moving vehicle in three directions: lift (up or down), lateral, and longitudinal (drag). They also act to generate pitch, yaw, and roll moments. In this work, and particularly for the purpose of the longitudinal motion equation, only the drag force is considered. The drag force is computed according to equation (9). The air density (ρ) in equation (9) varies with altitude and temperature according to equation (10).

$$F_{aero} = \frac{1}{2} \cdot \rho \cdot V^2 \cdot C_d \cdot A \tag{9}$$

$$\rho = 0.00236 \cdot \left(\frac{P_r}{29.92}\right)\left(\frac{520}{T_r}\right) \tag{10}$$

where:

- ρ is the air density (lb-sec^2/ft^4)
- V is the speed of the vehicle (ft/sec)
- C_d is air drag coefficient of the vehicle
- A is frontal area of the vehicle (ft^2)
- P_r is the current pressure at the altitude where the vehicle is operating (in-Hg)
- T_r is the ambient temperature (deg-Rankin)

Tire force characteristics

This simulation employs a tire model that relates traction force to slip. The longitudinal force generated by the tire is a complex function of the slip developed in the tire-road contact zone. That function is of the form described graphically in figure 7.

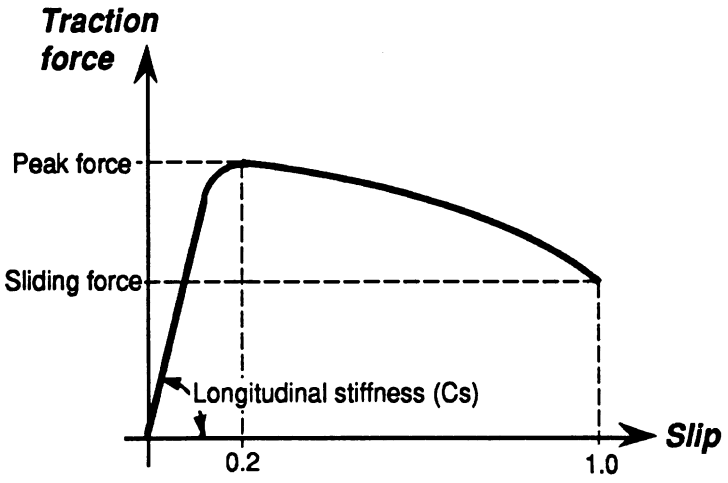

Figure 7. Longitudinal tire-force model

The slip is defined in terms of relative motion between the tire and the road surface on which it is rolling. From the typical curve in figure 7, it can be observed that some level of slip must be developed in order to generate traction force. Using the relationship between the circumferencial velocity of the rotating tire computed based on its rotational speed, and the forward speed of its hub, the slip can be expressed as:

$$s = 1 - \frac{2\pi \cdot \overline{\omega}_t \cdot R_t}{V} \tag{11}$$

where:

- s is the slip
- $\overline{\omega}_t$ is the rotational speed of the tire (rps)

R_t is the radius of the tire (ft)

V is the forward speed of the hub (the vehicle), (fps)

Starting at zero slip (a standstill tire with no drive forces applied), the traction force builds up approximately linearly with slip. This dependency prevails almost to the point of peak force, which is typically found in the neighborhood of 0.2 slip value. Beyond that level of slip, the traction force starts to decline until all the points in the contact patch are sliding. A slip of 1.0 is a lock-up braking situation.

Since a normal operation of vehicles in general and trucks in particular entails slip values of much less than those associated with peak force ($s << 0.2$), a linear relationship between slip and longitudinal tire force is assumed in the simulation. The linear coefficient, which is defined as the slope of the force/slip curve under zero slip (equation 12) is the longitudinal tire stiffness.

$$C_s = \left\langle \frac{\partial F_x}{\partial s} \right\rangle_{s=0} \tag{12}$$

where:

C_S is the longitudinal stiffness of the tire (lb)

F_X is the longitudinal force (lb)

The tire force generated by some value of slip can therefore be expressed as:

$$F_x = s \cdot C_s \tag{13}$$

Rolling resistance

The model employs the SAE equations for computing rolling resistance of heavy-truck tires (equations 14, 15). These equations are speed sensitive, and are distinguished by the tire type — radial or bias-ply.

$$F_{roll} = (0.0041 + 0.000041 \cdot V) \cdot C_r \qquad \text{(Radial)} \tag{14}$$

$$F_{roll} = (0.0066 + 0.000046 \cdot V) \cdot C_r \qquad \text{(Bias-ply)} \tag{15}$$

where:

V is the speed in mph

C_r is the road rolling coefficient; from 1.0 for a good road to 1.5 for a poor one

Engine torque

The engine model used in the simulation employs an approximation to characteristic power/torque performance curves. A typical engine power curve is portrayed in figure 8. Most diesel engines are intended to be used between the point of maximum torque and the point of peak power on their power curves. The model assumes a second order polynomial approximation to the torque curve within that operation range. When the engine speed is outside those boundaries, the torque is assumed to drop in a linear fashion. A comparison between such an approximation and actual engine performance data was found to be within satisfactory limits for the purpose of this simulation.

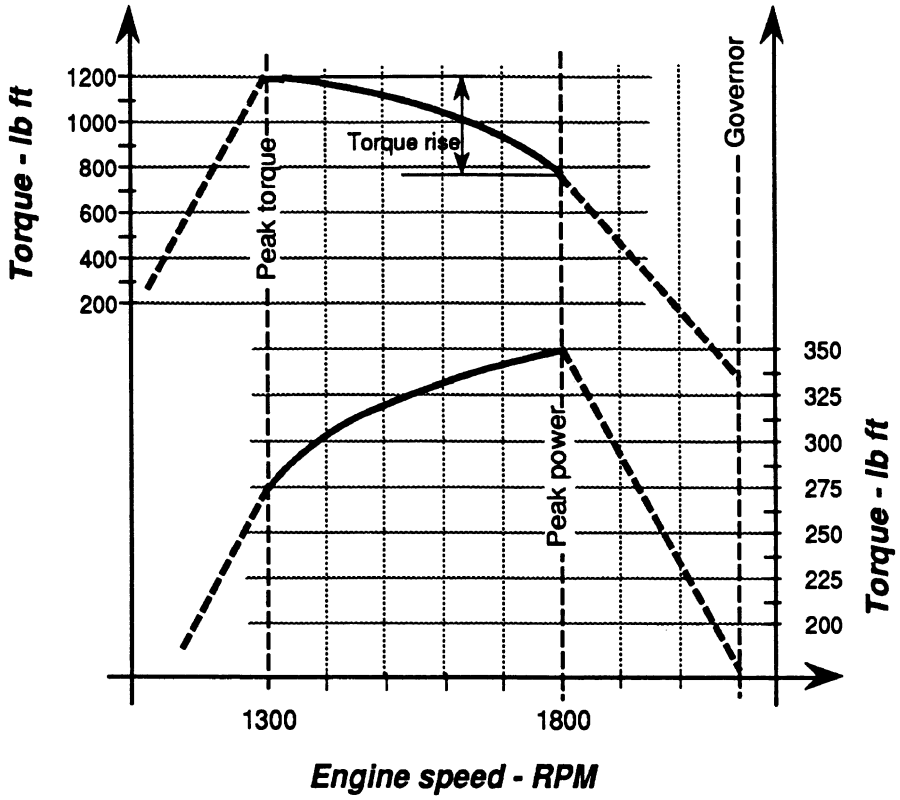

Figure 8. 350 hp diesel engine — typical power and torque curves

The equation for the approximated torque-curve polynomial is of the form:

$$T = A + B \cdot \omega_e + C \cdot \omega_e^2 \tag{16}$$

where:

A, B, C are the polynomial fit coefficients

ω_e is the rotational speed of the engine (rpm)

T is the fitted torque (lb ft)

From figure 8, it can be observed that the torque curve reaches a maximum at its peak (its derivative with respect to engine speed is zero). Such a peak phenomenon is typical to almost all diesel engines, with the exception of some two-stroke engines. It should be noted that such a statement (zero derivative at the peak) cannot be made regarding the power curve. Usually there is discontinuity in slope at the point of maximum power, and the derivative is not zero. Given two points on the curve (peak torque and its corresponding rpm, and the torque at peak power with its corresponding rpm), together with the *zero slope* relationship, the model computes the coefficients A, B, and C.

The resulting torque curve described by equation 16, which is the solid torque line in figure 8, pertains to a full-throttle situation. Partial-throttle torque is computed by proportioning the full-throttle value computed by equation 16. During the simulation, equation 16 and the throttle proportioning are used to compute the gross engine torque (T_{gross} in figure 6) as follows:

$$T_{gross} = \left(A + B \cdot \omega_e + C \cdot \omega_e^2\right) \cdot \delta_t \tag{17}$$

where:

T_{gross} is the computed engine torque based on engine speed and throttle (lb ft)

δ_t is the throttle setting ("0" for closed, "1" for full throttle)

Torque lag

The thermodynamic processes associated with the combustion, and the dynamics of the internal engine parts are introduced to the engine model in a simplified form of a time lag. This time lag (τ_e) is defined as the rate of torque development. Under a given set of conditions (ω_e, δ_t) the resulting engine torque as expressed by equation 17 and illustrated in figure 8 is not produced instantaneously. A time constant (τ_e) is required for the torque to progressively develop from its current value to its newly computed (T_{gross}) value. That relationship is expressed by equation 18.

$$\dot{T}_e = \left(T_{gross} - T_e\right) \cdot \frac{1}{\tau_e} \tag{18}$$

where:

T_e is the current engine torque (lb ft)

$\dot{T}_e$ is the engine torque rate (lb ft /sec)

Torque losses

Motoring losses in the engine that are considered in this work are those associated with friction and accessories. Furthermore, since the model that was constructed and studied in this work focuses on heavy trucks, the following torque losses model pertains to diesel engines. Losses due to both friction and accessories for a spark-ignition engine will require a different modeling method.

In a study titled "Frictional Losses in Diesel Engines" [8], several friction related factors were looked into (rings, viscosity, pumping, etc.). After experience with various engine designs and sizes, the authors suggested the empirical relationship presented in equation 19. The curve described by this equation was compared with data collected from modern design engines, and was found to provide a sound empirical correlation.

$$P_{emp_{loss}} = A + 7 \cdot \frac{\omega_e}{1000} + 1.5 \cdot \left(\frac{\mathcal{V}_p}{1000} \right)^2 \tag{19}$$

where:

$P_{emp_{loss}}$	is the mean effective pressure motoring losses (psi)
A	is the compression ratio (CR) for indirect injection diesel engines, and the compression ratio minus 4 (CR-4) for direct-injection diesel engines
ω_e	is the engine speed (rpm)
$\mathcal{V}_p$	is the mean piston speed at ω_e (fpm)

Friction losses in the engine as computed by equation 19 are in terms of mean effective pressure. These losses can be expressed in terms of torque by using the following relationship [9]:

$$T_{friction} = 0.00662954 \cdot P_{emp_{loss}} \cdot V_H \tag{20}$$

where:

$T_{friction}$	is the torque motoring losses (lb ft)
V_H	is the engine volume (in^3)

Accessories' torque loss is estimated to be 5% of the gross engine torque. The expression for the total torque losses in the engine can therefore be written as:

$$T_{loss} = T_{friction} + 0.05 \cdot T_{gross} \tag{21}$$

Rotational degree of freedom

The differential equation for the rotational degree of freedom in the vehicle model relates to the torque and the rotating inertias of the powertrain. Inertia properties of the engine, transmission, and wheels play an important role when considering acceleration capabilities of the vehicle. In fact, in the lower gears, more engine torque is delivered to accelerate those rotating inertias than to accelerate the vehicle. The rotational motion of the powertrain inertias is described by the following differential equation:

$$I_e \cdot \dot{\omega}_e = \eta_v \cdot T_e - \frac{T_t}{\eta_d} - \frac{I_d \cdot \dot{\omega}_e}{(i_{ax} \cdot i_g)^2} - T_{loss} \qquad (22)$$

where:

I_e is the rotational inertia of the engine (lb ft sec^2)

$\dot{\omega}_e$ is the rotational acceleration of the engine (rad /sec /sec)

η_v is the volumetric efficiency of the engine

T_e is the current engine torque (lb ft)

T_t is the engine torque needs to the drive the wheel, based on tire force (lb ft)

η_d is the efficiency of the drive train

I_d is the combined inertia of the transmission and wheels (lb ft sec^2)

i_{ax} is the gear ratio of the rear axle

i_g is the gear ratio selected in the transmission

T_{loss} is the torque motoring losses (lb ft)

An empirical approximation suggested in [10] to compute engine inertia, is given in equations (23),(24):

$$I_e = \frac{1}{32.2} \cdot \left[4 + 1.2 \left(\frac{V_H}{100} \right)^2 \right] \qquad \text{(V type gasoline engines)} \qquad (23)$$

$$I_e = \frac{1}{32.2} \cdot \left[4 + 1.6 \left(\frac{V_H}{100} \right)^2 \right] \qquad \text{(In-line gasoline and four cycle Diesel)} \qquad (24)$$

4.0 SIMULATION RESULTS

A computer simulation of the headway-control system with the vehicle model as described in the previous sections was developed and exercised. In this section, outputs of two simulation runs are presented and discussed: first, the response of the system operating at cruise-control mode to a grade disturbance; second, the system-switching function is analyzed as it transitions from cruise- to headway-control mode and back, as a traffic

disturbance enters and leaves the simulated scene. Experimenting with the model, in general, and with these examples in particular, reveals features that are desirable for later inclusion in the simulation.

4.1 Grade disturbance

This example simulates a situation where the truck, while being operated under cruise control, negotiates a 3% grade disturbance. The data set that describes the simulated truck, as needed for input to the computation, is provided in Appendix A. Note that those parts of the data that pertain to a leading vehicle (e.g., speed table, distances, times, etc.), are not used in this example since the simulated truck is assumed to be far behind any leading vehicle, and therefore operates in an uninterrupted cruise-control mode.

The 3% grade disturbance is introduced in a gradual manner. It is shown graphically in figure 9 (which is a representation of the road profile data in Appendix A).

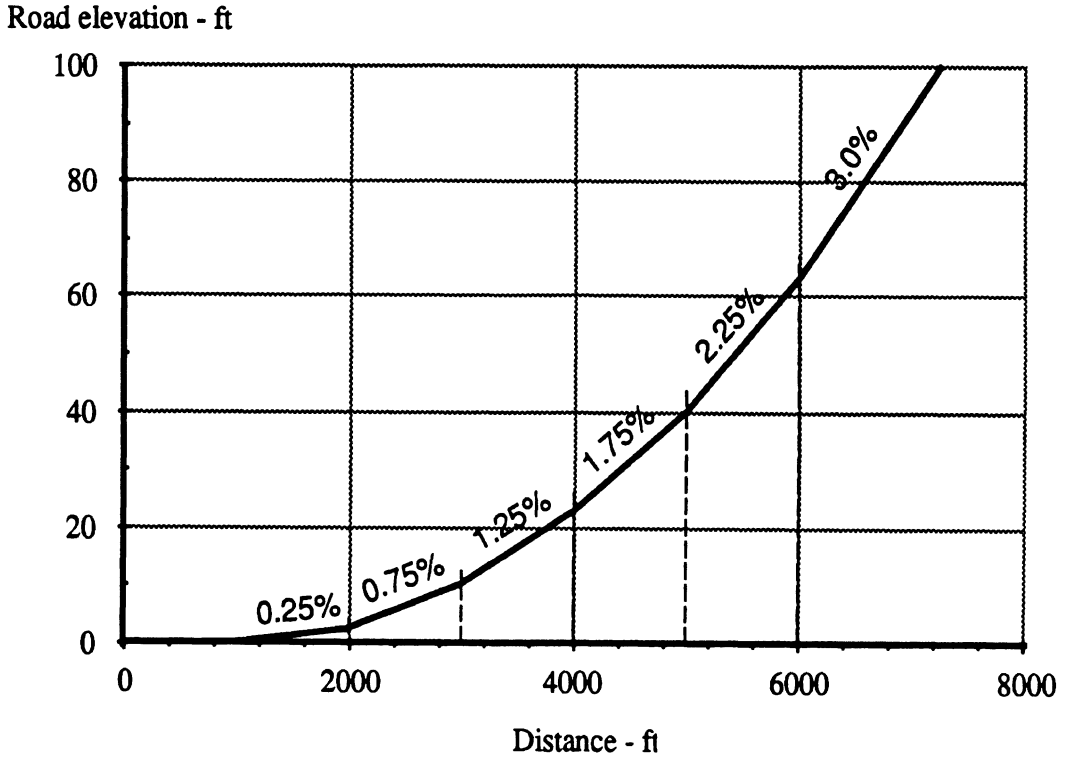

Figure 9. Gradual 3% grade profile

The response of the system to the grade disturbance is described in figures 10 through 12. Initially, the truck cruises on the level road at a steady state speed of 43.8 mph. Other

corresponding equilibrium parameters under these conditions are 0.5 throttle setting, and an equivalent total slip of 0.058 at the tires. As the truck encounters the various grade stages, the cruise-control system acts to compensate for the disturbances by increasing the throttle accordingly. The added torque generated by the engine to compensate for the increased resistance force is translated to traction force in the tires through increased slip.

The results of the simulation indicate that the 50,000-lb truck will travel up the 3% grade at full throttle, while maintaining a steady-state speed of 43.5 mph, a negligible speed loss from the level-road, steady-state speed. The slip that the tires need to develop to provide the added tractive force is 0.135, which is over twice the slip for a steady-state motion on a level road.

Currently, the model does not have gear-changing capability. The truck must be able to handle the disturbances while keeping the same gear ratio throughout. If the engine speed computation results are either above the maximum rated speed, or below a minimum (900 rpm), the simulation terminates.

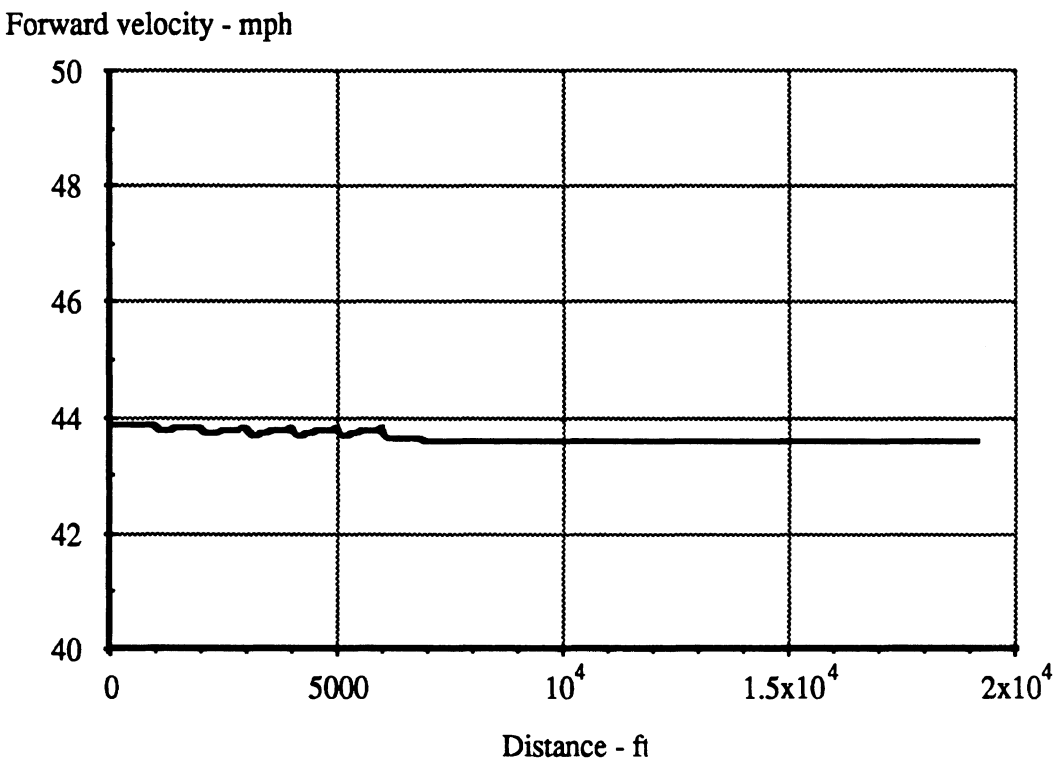

Figure 10. Speed response to grade disturbance

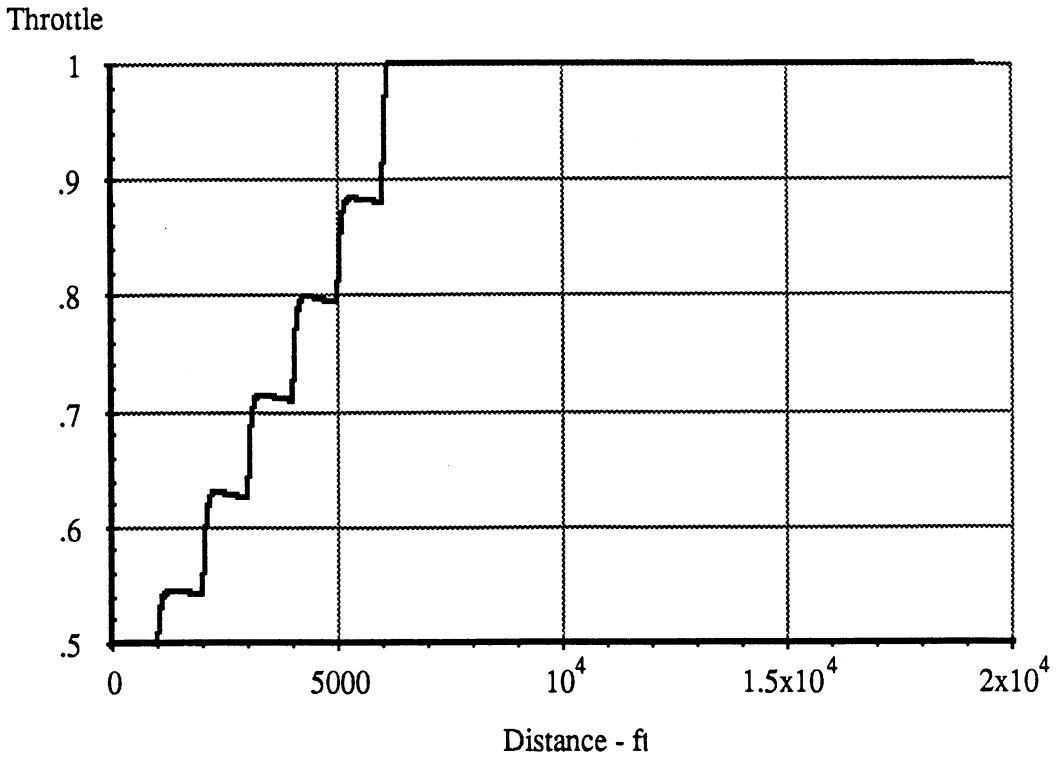

Figure 11. Throttle response to grade disturbance

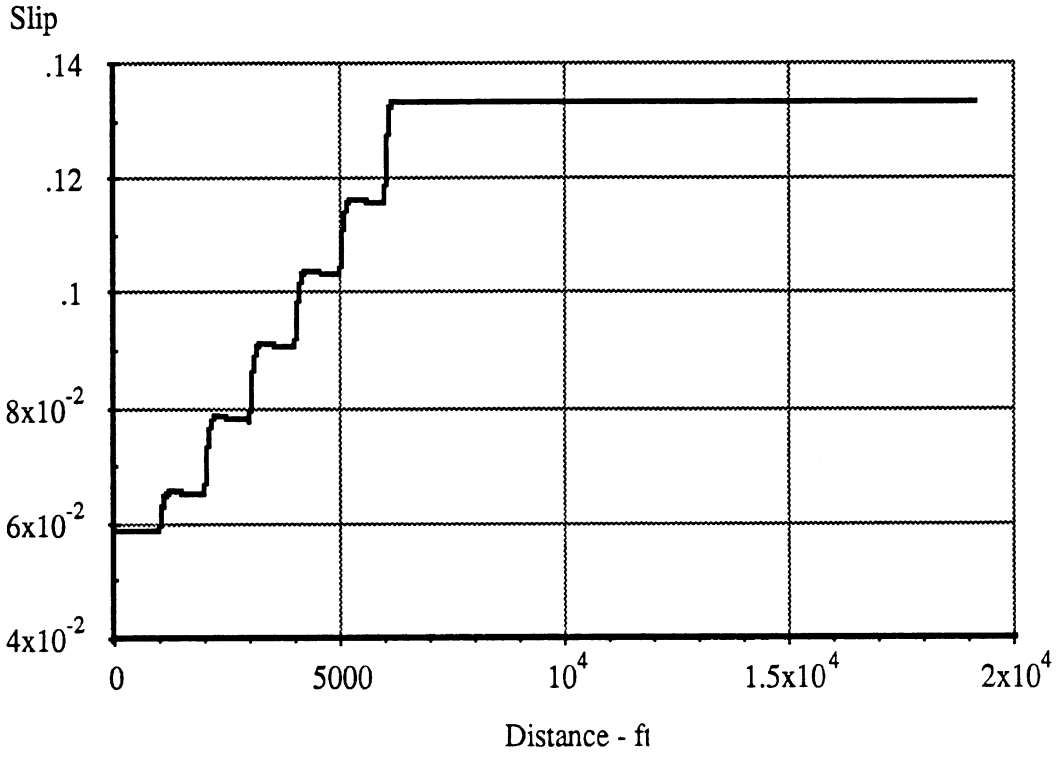

Figure 12. Total tires slip on a 3% grade

4.2 Leading-truck disturbance

In this example, a dynamic interaction between two vehicles is simulated. This case is more complex than the grade disturbance example, since the controlling system needs to adapt to speed variations, as well as to switch operating modes. The data set that describes the simulated truck, as needed for input to the computation, is provided in Appendix B. The disturbing inputs (timings and the leading truck position) are also provided in that data set.

The simulated truck operates initially under cruise-control mode at 55.5 mph, 500 ft behind a leading vehicle, which is being driven at 50 mph. The speed of the leading vehicle varies with time as shown in figure 13. The response of the simulated truck to speed variations of the leading vehicle and the computational results are presented in figures 14 through 18. In the following discussion of the simulation results, points of interest are correspondingly marked in the figures and in the text.

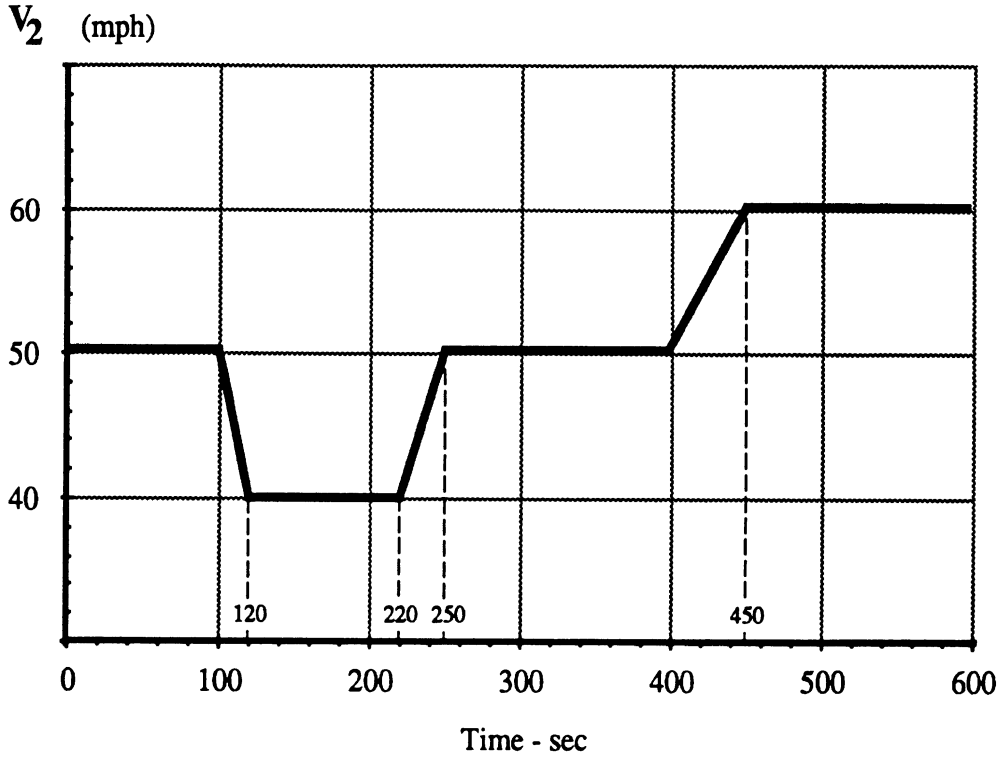

Figure 13. Leading-vehicle speed profile

Since it travels at a higher speed, the simulated truck closes the distance (range) to the vehicle ahead. At a certain point, the heuristic algorithm of the system switches from

cruise- to headway-control mode of operation ① (see figure 14). After the system's response is stabilized, the headway between the vehicles is about 140 ft, and the trailing vehicle tracks the leading one at 50 mph ②. This situation is maintained until the leading vehicle slows down to 40 mph. The headway-control system attempts to maintain the range by throttle commands, but the sluggish response of the heavy truck brings the range down to less than 100 ft when the system is stabilized ③ (see figure 16). This range is maintained, and the trailing truck tracks the speed of the leading vehicle (40 mph). At $t = 220$ sec, the leading vehicle accelerates back to 50 mph. The system responds, and when it is stabilized the range is 170 ft, and both vehicles are moving at 50 mph ④. At $t = 400$ sec ⑤, the leading vehicle starts accelerating to 60 mph, and it attains this speed at $t = 450$ sec. At first, the trailing truck increases its speed to follow the first vehicle, but in spite of a full throttle position (see figure 15), it cannot accelerate as fast. In figure 17, the plotted line departs point ⑤, indicating increased range and range-rate between the vehicles. As this line crosses the *switching line* ⑥, the system switches back to cruise-control mode. That event takes place at a range of 230 ft between the vehicles (figure 17), and at $t \approx 430$ sec (figure 16). The trailing truck is now still accelerating under full throttle, but the goal is the speed set initially by the driver (55.5 mph), and not the speed of the leading vehicle. When that speed is attained ⑦, it stabilizes (figure 14), and so do the throttle and the engine speed (figures 15, 18). Except for some transitioning effect (between points ⑦ and ⑧ in figure 17), the range now grows at a constant rate. Since the leading vehicle travels at a constant speed of 60 mph and the trailing truck travels at a constant speed of 55.5 mph, the range between them increases at a constant rate of 4.5 mph as shown in fig. 17 beyond point ⑧ by the vertical line at a 4.5 mph range rate.

Sensitivity to weight variation was the next aspect of system performance that was evaluated. As shown in the data in Appendix B, the simulated trailing truck weighed 80,000 lb. Exercising the simulation with a 30,000-lb truck would allow for a qualitative assessment of the system's performance when used under both fully loaded and empty conditions. For comparison, the results of the 30,000-lb simulation are portrayed in figures 19 through 23, combined with those for the previous 80,000-lb run.

The first observation from the figures is that the system performs rather adequately under both loaded and empty conditions. Comparing figures 15 and 20 also shows that the throttle setting required to maintain a cruising speed of 55.5 mph is 0.9 when loaded to 80,000 lb, but it is only 0.76 with 30,000 lb. Throughout the simulation, the throttle

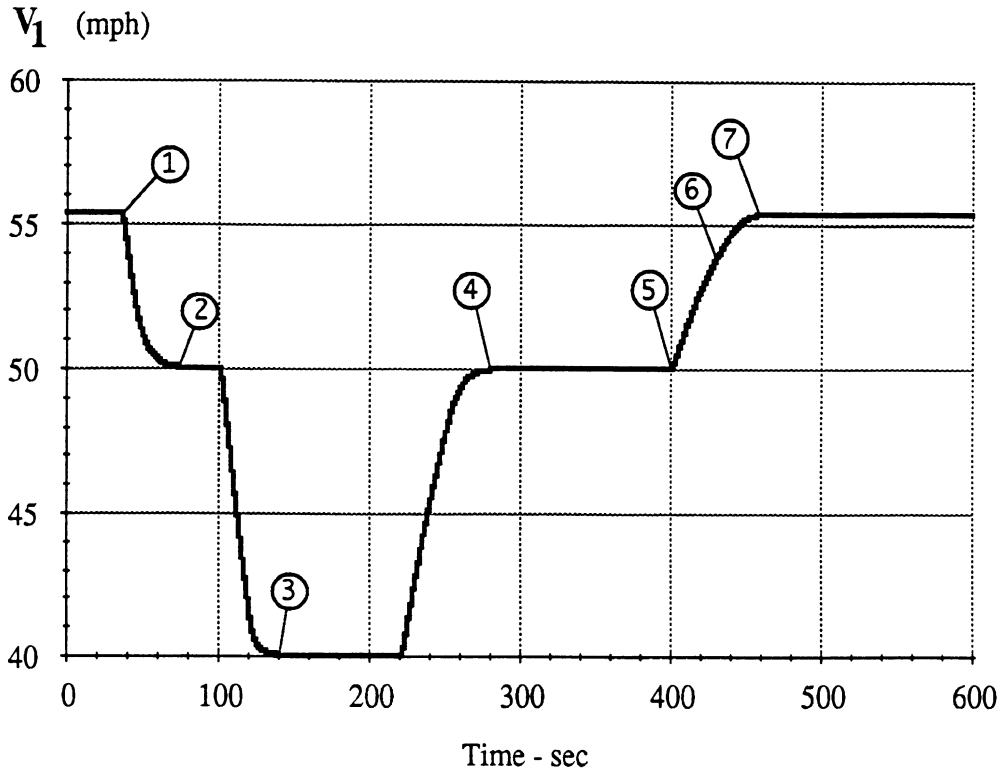

Figure 14. Speed response of the trailing truck

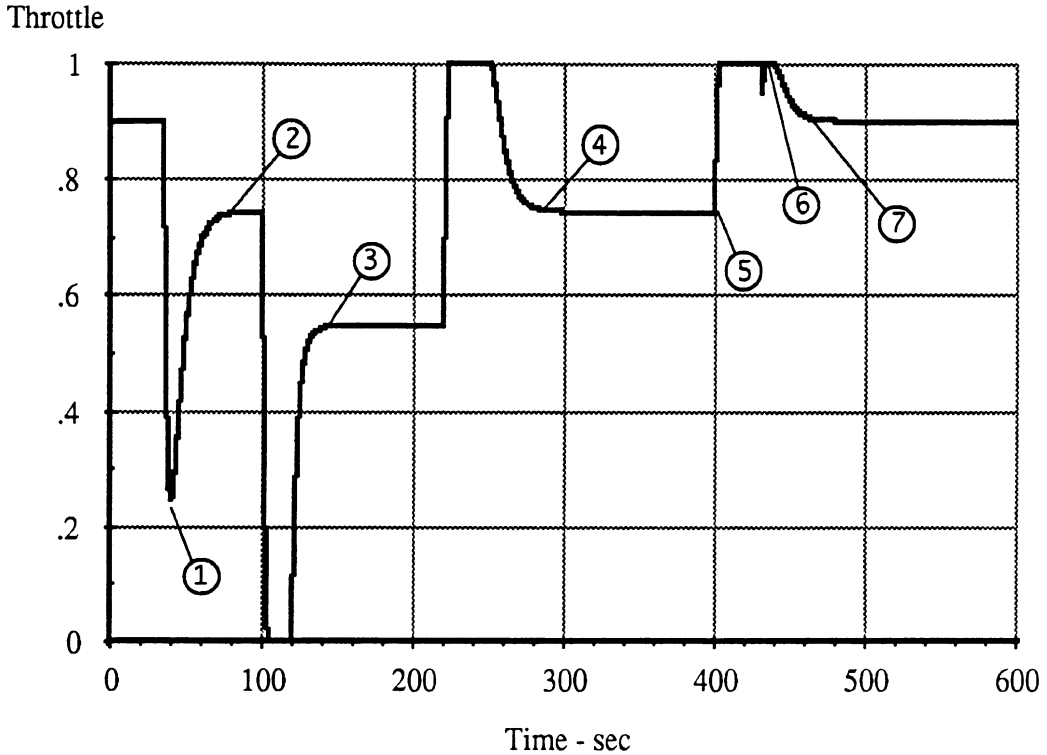

Figure 15. Throttle response of the trailing truck

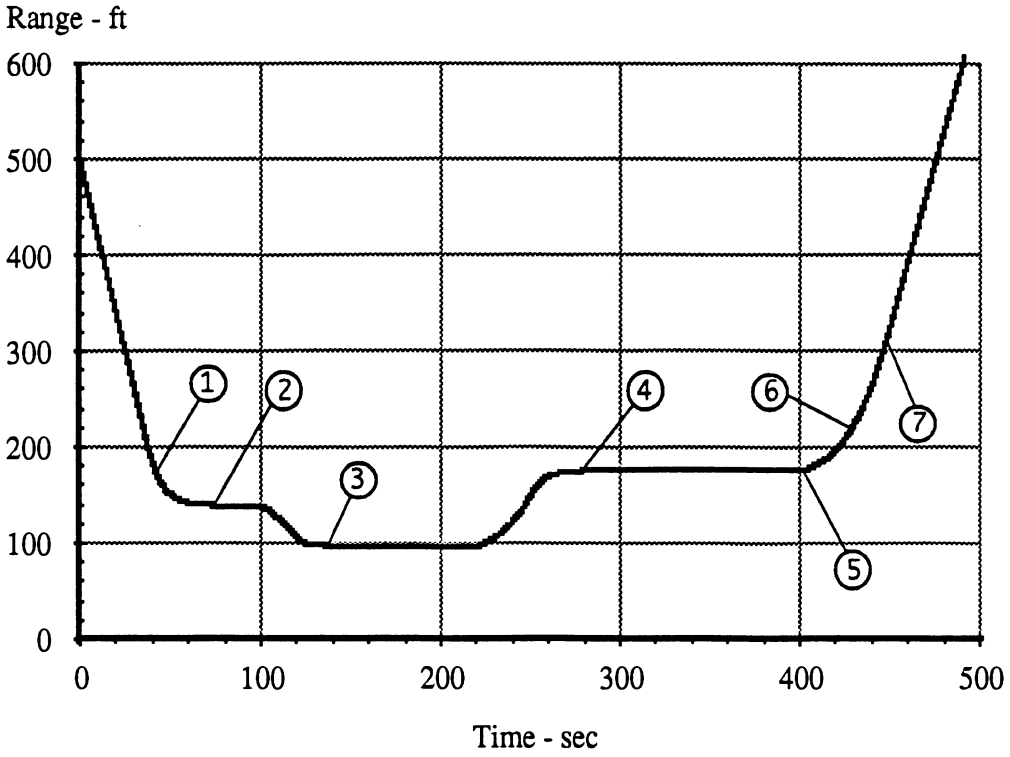

Figure 16. Range between leading and trailing vehicles

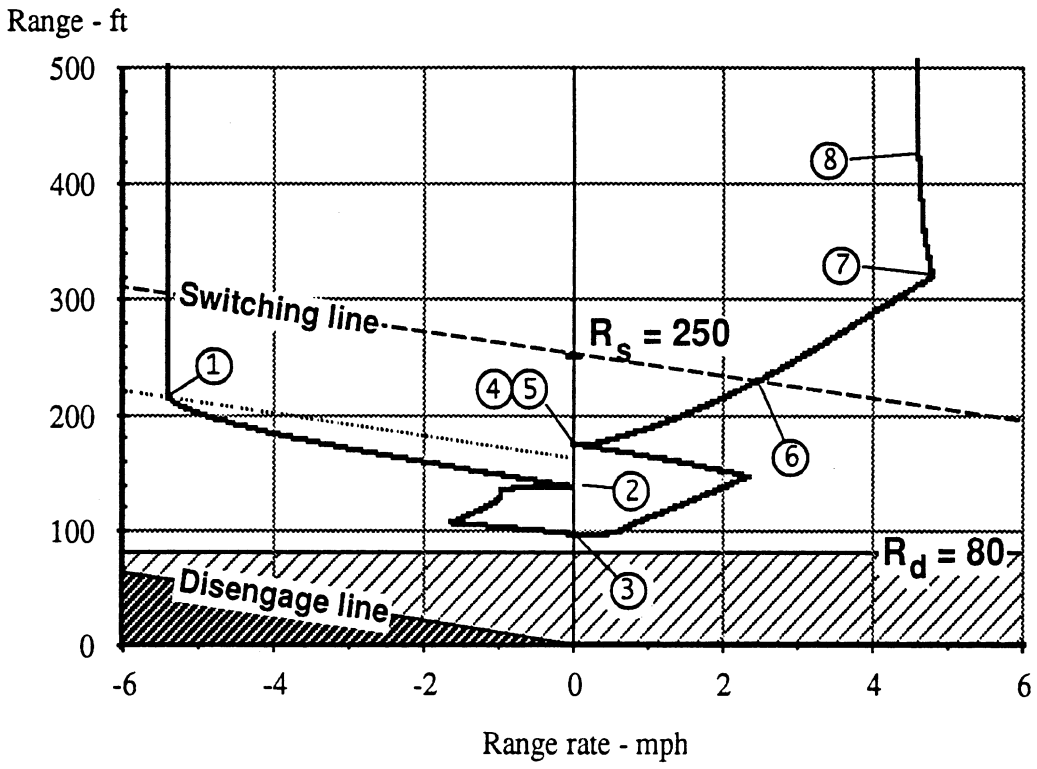

Figure 17. Range and range rate, overlaid on headway control algorithm

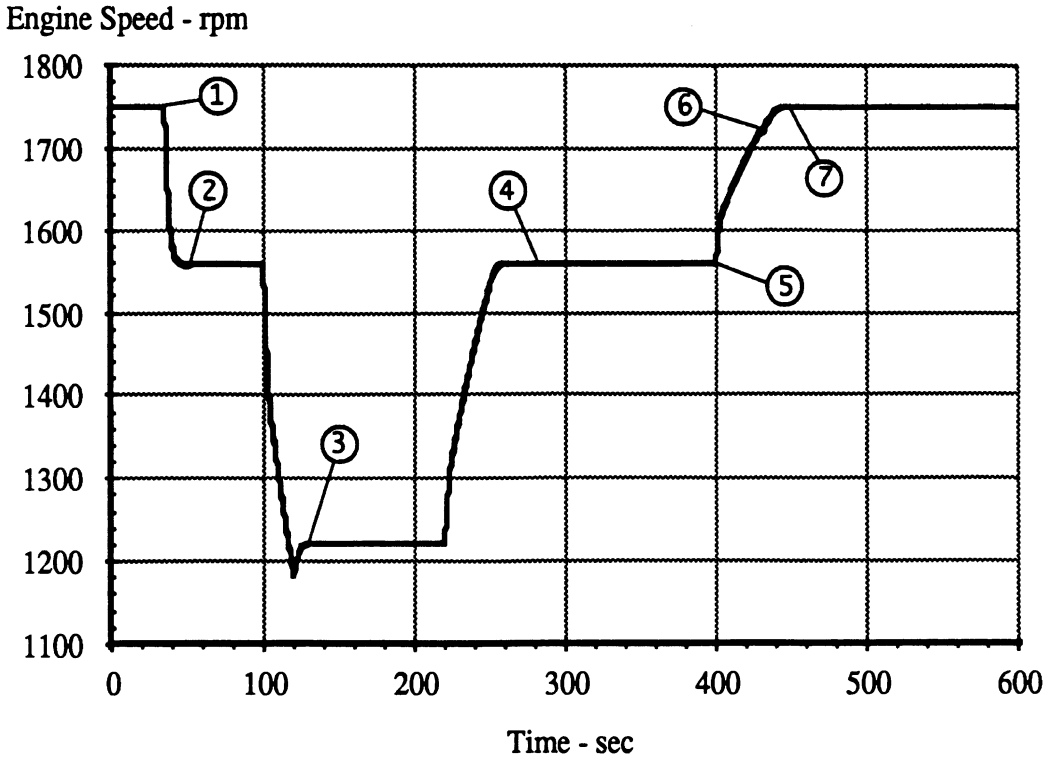

Figure 18. Simulated engine-speed response

motions to adjust the speed are also much smaller. During the headway-mode operation (between approximately 50 sec and 400 sec), the range in figure 21 was better maintained, and adjustments were made quicker with a weight of 30,000 lb. In figure 22, the "loop" portions of the plot that represent the response delay (relative motion between the vehicles while the system stabilizes back to zero range rate), are much tighter for the 30,000-lb case due to the quick response. Finally, there are small differences in engine speed between the 80,000-lb and 30,000-lb vehicles as illustrated in figure 23. As discussed in the model description section, the traction force is computed by the tire model based on the amount of slip (see figure 7 and equation 11). The higher the slip, the larger is the traction force. Observing figures 19 and 23, during the periods of constant speed motion (approx. 50-100 sec, 130-220 sec, 250-400 sec, and after 450 sec), with 30,000 lb the engine speed was always lower than with 80,000 lb. Since the truck was moving at the same speed in both cases, equation 11 indicates that the slip was lower with 30,000 lb, therefore the traction force required to drive the lighter truck was lower.

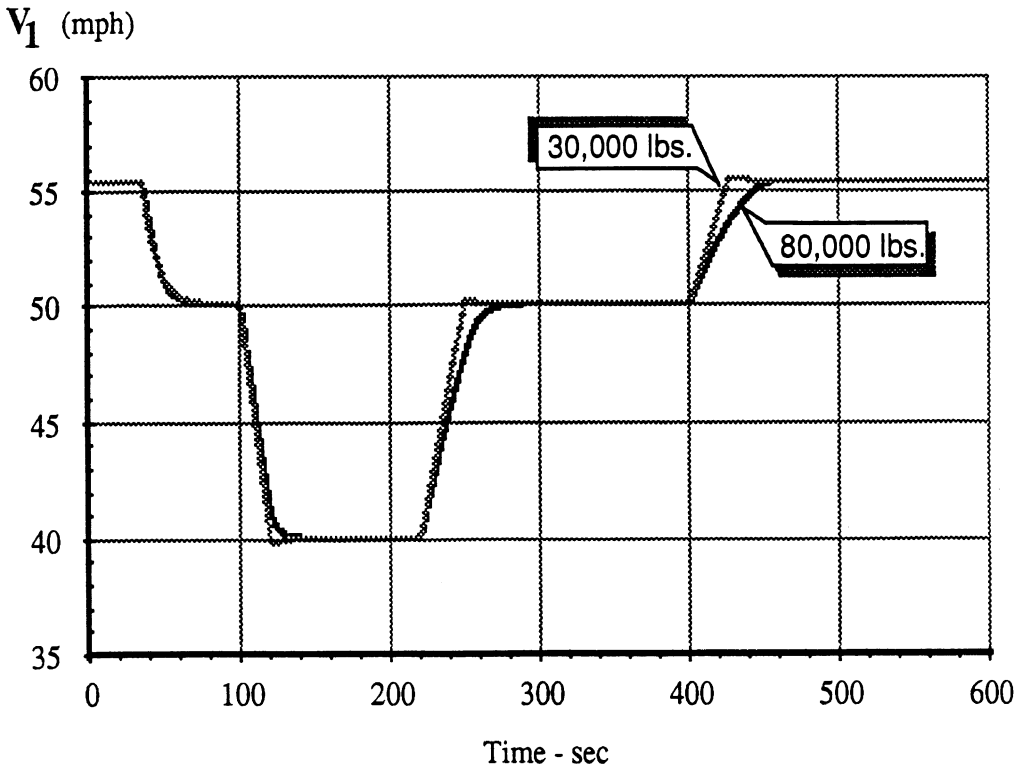

Figure 19. Speed response comparison — 80,000 lb vs. 30,000 lb

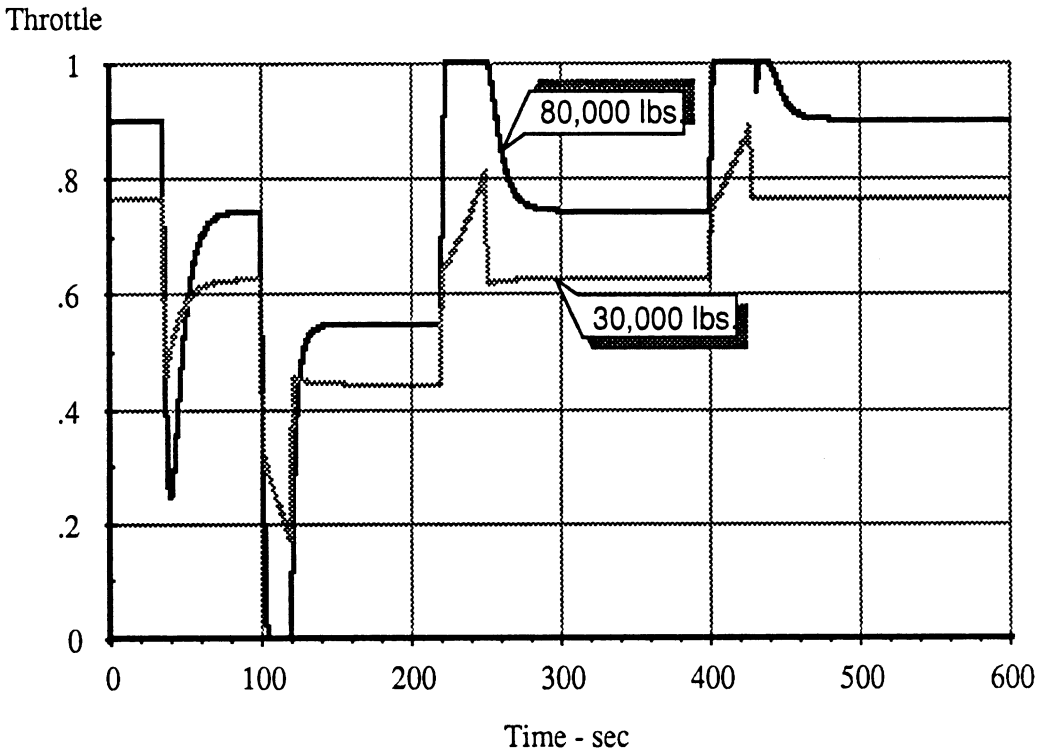

Figure 20. Throttle response comparison — 80,000 lb vs. 30,000 lb

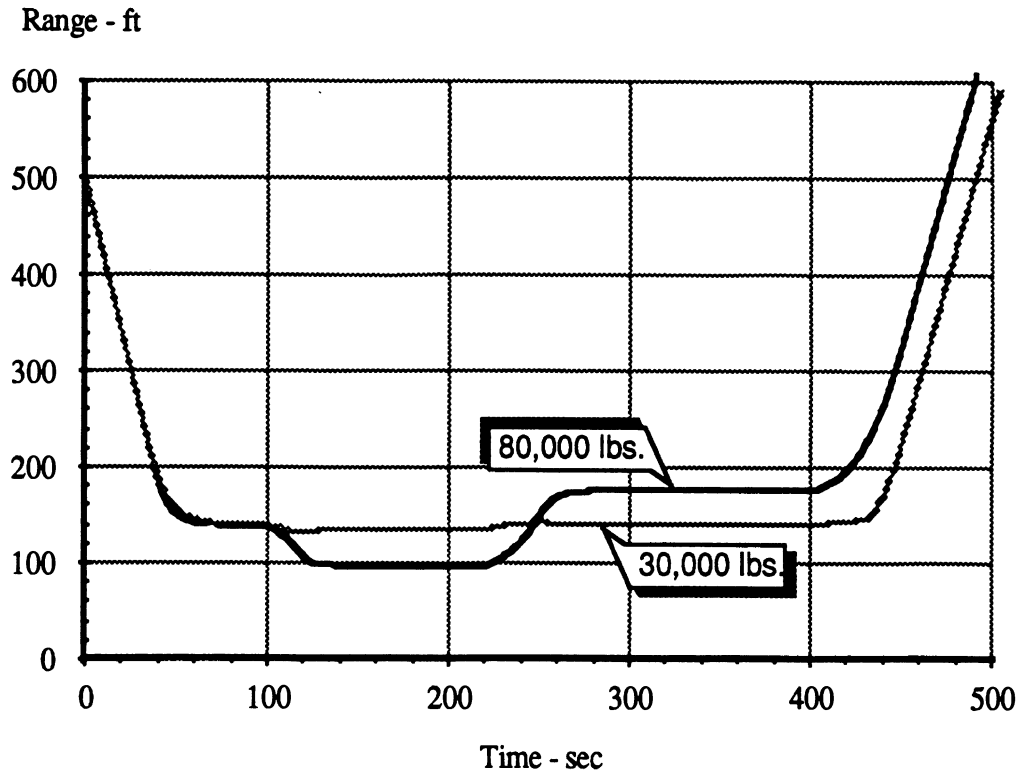

Figure 21. Range between the leading vehicle and the trailing truck under different loads

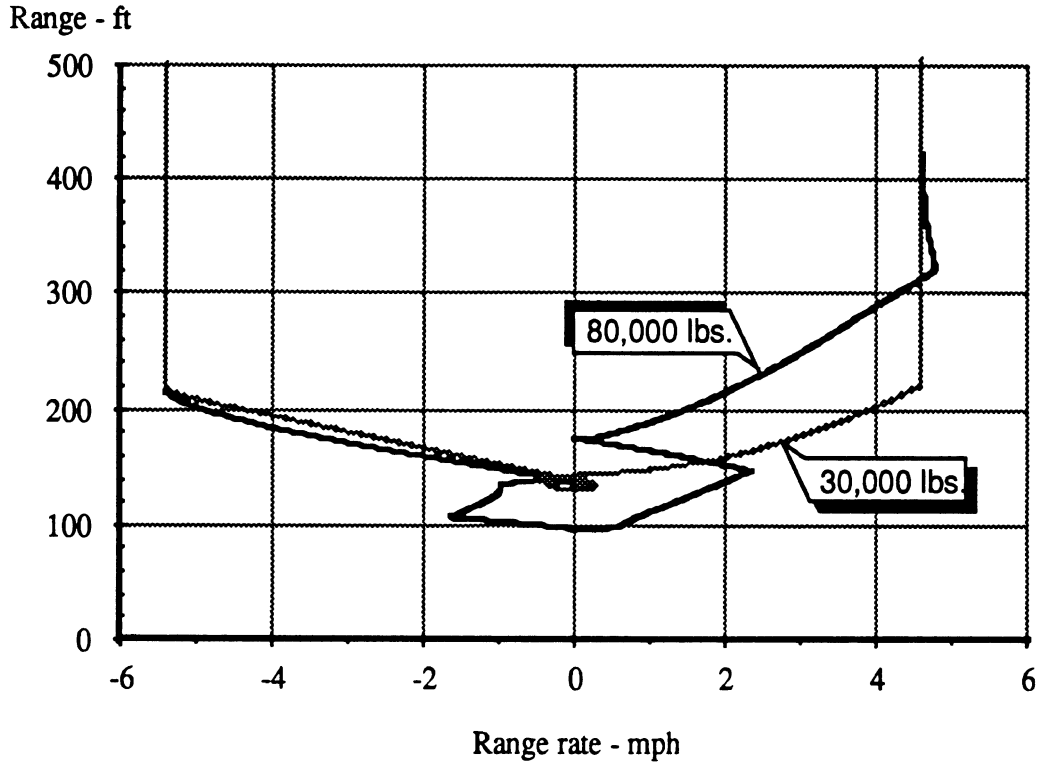

Figure 22. Range and range-rate between the leading vehicle and the trailing truck under different loads

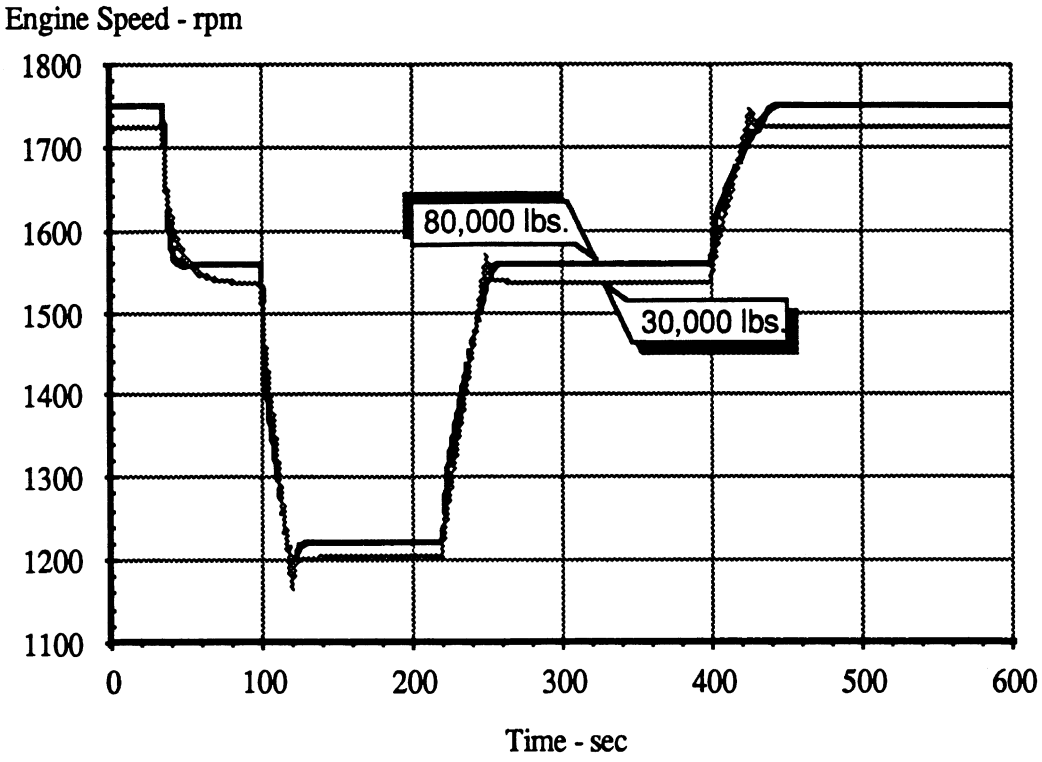

Figure 23. Engine-speed response comparison — 80,000 lb vs. 30,000 lb

As described above and illustrated by figures 16, 17, 21, and 22, there is a lag in the response of the trailing truck for speed changes of the leading vehicle. That lag is especially pronounced when the trailing truck is heavily loaded. In figure 17, the section of the plot between point ② and point ③ demonstrates this sluggish response. Point ② represents motion while a constant headway is maintained (constant speed, zero range-rate). Point ③ represents another such stabilized motion. Between these two points the leading vehicle slowed down from 50 to 40 mph. The plot shows that the trailing truck gets closer to the leading vehicle (negative range-rate with a decreasing range) due to a slow response time. Had the leading vehicle slowed down again, the plot would have cut below the minimum range line (R_d), and the system would have been disengaged. To prevent such situations of unnecessary system disengagement, a *backing-off* feature should be incorporated into the system. With this feature, when the system is stabilized and a constant headway is maintained, the trailing vehicle would slow down momentarily to increase the headway to some nominal value. That feature is planned to be incorporated into the system in future stages of the work.

5.0 SIMULATION INCORPORATING CONTROL HARDWARE

Unlike the simulation described so far, which is a mathematical model computed in the "sealed" environment of a computer, the field experiment that is planned will entail the use of some hardware items to control the headway of the test truck. In order to affirm the feasibility of implementing headway control in trucks, and to take a further step towards a realistic field experiment, the simulation was modified so as to incorporate those hardware items that were available at this stage.

During the headway-control experiment, the following hardware items will be installed in the test truck:

1. Control unit
2. Headway parameters adjustment panel
3. Range and range rate sensors

The control-unit switches between the cruise- and the headway-control modes of operation according to the heuristic algorithm described in section 3.1. Such a control unit was built, and a set of four potentiometers were also assembled so as to make the headway parameters adjustment panel. An additional potentiometer was used to set the cruising speed as it might be selected by the driver. Since this set of hardware is intended to be used in the experiments, it was desirable to validate its functionality before actually installing it in the vehicle, although at that stage the range sensors were not yet available for experimentation. The simulation was then redesigned to represent the truck and the missing sensors, and to be able to "communicate" with the set of the control hardware items.

Currently, the simulation performs the calculations while successfully communicating with the control hardware. A range / range-rate plot that depicts the system's settings and its real-time response is displayed on the screen (see figure 24), and the relative motion of the truck and the lead vehicle is also animated. The user can observe the actual response of the truck, and monitor the operation of the system by modifying the headway-control parameters at any time. During the field tests that are planned, the driver of the truck will be able to modify the four headway-control parameters and to change the speed of the cruise control while monitoring on a screen the real-time range and range-rate status between the two vehicles.

The real-time display will aid in monitoring the process and will facilitate the evaluation of the performance of the headway-control system. Results of the simulation that

incorporates the control hardware were validated by having it perform calculations similar to the example runs in section 4.0, but with the appropriate parameters being set externally.

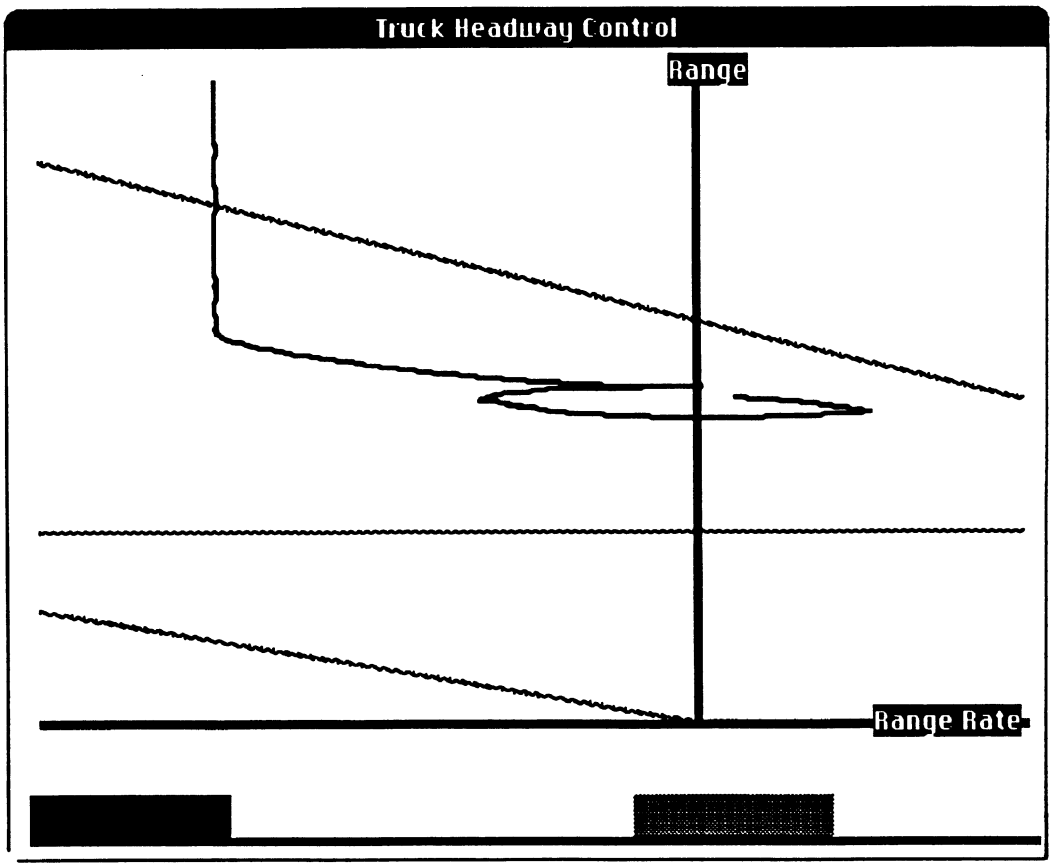

Figure 24. Real-time screen display

6.0 CONCLUSION

Through computer simulation, an intelligent cruise-control system for use on heavy-duty trucks has been defined and its perfomance studied. The simulation results indicate that at least theoretically, the system performs as predicted, and it can be made to perform satisfactorily.

The concept of headway control developed here implements the cruise-control system of the vehicle, while extending its functionality. The headway-controlled vehicle maintains its autonomous nature in traffic, yet, an adaptive control function is exercised as headway clearances reduce. The end result of incorporating headway-control systems into the traffic pattern is enhanced safety, fuel saving via extending the usable envelope of the cruise control, and reduction in the workload on the driver.

In addition to topics that are related to vehicle and traffic engineering, the headway-control system in its current configuration can be used to study issues that pertain to human factors. The ability to adjust the headway-control parameters and to experiment with all the possible settings of the system allows one to substantiate various "comfort zones." Human performance in such situations of leading-trailing vehicles can then be studied and compared with those of more completed automated operations.

It is still necessary to address the issues of the unknown sensors hardware and the challenge involved in accurately measuring range and range-rate within a fully functional and integrated experimental system. However, such issues could be resolved only by carrying out an actual field test.

At this point, based on the results obtained so far, we are confident that such a system is feasible. The desired next step is conducting experiments with the system installed in a heavy truck.

REFERENCES

1. Miyata, Y., et al. "Present and Future of Cruise Control Systems," *JSAE Review*, Vol. 11, No. 3, July 1990, pp 37-44.

2. Liubakka, M. K., Winkelman, J. R., and Kokotovic, P. V. "Adaptive Automotive Speed Control," *Proceeding of the American Control Conference*, Boston, Mass., June 1991, pp 439-440.

3. Tsujii, M., Takeuchi, H., Oda, K., and Ohba, M. "Application of Self-Tuning to Automotive Cruise Control," *Proceeding of the American Control Conference*, San Diego, California, May 1990, pp 1843-1848.

4. Ulsoy, G. A. Notes from a presentation at the IVHS Industrial Advisory Board Meeting, January 10, 1991, Department of Mechanical Engineering and Applied Mechanics, The University of Michigan, Ann Arbor, Michigan.

5. Cho, D., and Hedrick, J. K. "Automotive Powertrain Modeling for Control," *Journal of Dynamic Systems, Measurements and Control*, Vol. 111, December 1989, pp 568-576.

6. Jeffery, A., et al. "Modeling of an Internal Combustion Engine for Control Analysis," *IEEE Control Systems Magazine*, August 1988, pp 20-25.

7. Ford, M. P. "A Simplified Turbocharged Diesel Engines Model," *Proceedings of the Institute of Mechanical Engineers*, Vol. 201, No. D4, 1987, pp 229-234.

8. Millington, B. W., and Hartles, E. R. *Frictional Losses in Diesel Engines*, SAE Paper 680590, Sept. 1968.

9. *Bosch Automotive Handbook*, 18th German edition, 1st English edition, 1978, Distributed by SAE, USA.

10. Smith, G. L. *Commercial Vehicle Performance and Fuel Economy*, (the 16th L. Ray Buckendale Lecture), SAE SP-355, New York, January 1970.

APPENDIX A

Input file for grade disturbance run

1.	Gross combination weight (lb)	50000
2.	Load on driving axle(s) (lb)	30000
3.	Tire radius (ft)	1.8
4.	Longitudinal tire stiffness (lb)	20000
5.	Polar moment of inertia for driveline (ft-lb-sec^2)	175
6.	Polar moment of inertia for engine (ft-lb-sec^2)	3.5
7.	Frontal area of the vehicle (ft^2)	100.
8.	Drag coefficient (aerodynamic)	.9
9.	Road coefficient (rolling resistance)	1.
10.	Rear axle ratio	4.11
11.	Gear ratio	1.1
12.	Maximum engine torque (ft-lb-sec^2)	1325.
	at speed (RPM)	1300.
13.	Engine torque at max power point (ft-lb-sec^2)	1167.
	at speed (RPM)	1800.
14.	Maximum no-load governed engine speed (RPM)	2300
15.	Engine volume (cu.in.)	855.
16.	Piston stroke (in.)	6.
17.	Compression ratio	20.
18.	Engine volumetric efficiency	0.93
19.	Drivetrain efficiency	0.95
20.	Road friction limit	0.9
21.	Simulation stop time (sec)	300.
22.	Engine lag (sec) (≈0.1 if non-turbo,≈1.5 if turbo)	.1
23.	Initial range from leading vehicle (ft)	2500.
24.	Minimum acceptable range from leading vehicle (ft)	80.
25.	Range from lead vehicle to switch mode (ft)	250.
26.	Time too short boundary slope (sec)	7.
27.	Mode switch boundary slope (sec)	7.
28.	Number of points in road profile	8
29.	Number of points in leading vehicle speed table	2

Road profile table:

	Distance (ft)	Elevation (ft)
1.	0.	0.
2.	1000.	0.
3.	2000.	2.5
4.	3000.	10.
5.	4000.	22.5
6.	5000.	40.
7.	6000.	62.5
8.	20000.	482.5

Leading vehicle speed table:

	Time (sec)	speed (mph)
1.	0	60.
2.	100	60.

APPENDIX B

Input file for a leading-truck disturbance run

1.	Gross combination weight (lb) ----------	80000
2.	Load on driving axle(s) (lb) ----------	30000
3.	Tire radius (ft) ----------	1.8
4.	Longitudinal tire stiffness (lb) ----------	20000
5.	Polar moment of inertia for driveline (ft-lb-sec^2) ---	175
6.	Polar moment of inertia for engine (ft-lb-sec^2) ------	3.5
7.	Frontal area of the vehicle (ft^2) ----------	100.
8.	Drag coefficient (aerodynamic) ----------	.9
9.	Road coefficient (rolling resistance) ----------	1.
10.	Rear axle ratio ----------	4.11
11.	Gear ratio ----------	.9
12.	Maximum engine torque (ft-lb-sec^2) ----------	1325.
	at speed (RPM) ----------	1300.
13.	Engine torque at max power point (ft-lb-sec^2) --------	1167.
	at speed (RPM) ----------	1800.
14.	Maximum no-load governed engine speed (RPM) ----------	2300
15.	Engine volume (cu.in.) ----------	855.
16.	Piston stroke (in.) ----------	6.
17.	Compression ratio ----------	20.
18.	Engine volumetric efficiency ----------	0.93
19.	Drivetrain efficiency ----------	0.95
20.	Road friction limit ----------	0.9
21.	Simulation stop time (sec) ----------	600.
22.	Engine lag (sec) (≈0.1 if non-turbo,≈1.5 if turbo) ----	.1
23.	Initial range from leading vehicle (ft) ----------	500.
24.	Minimum acceptable range from leading vehicle (ft) ----	80.
25.	Range from lead vehicle to switch mode (ft) ----------	250.
26.	Time too short boundary slope (sec) ----------	7.
27.	Mode switch boundary slope (sec) ----------	7.
28.	Number of points in road profile ----------	2
29.	Number of points in leading vehicle speed table -------	8

Road profile table:

	Distance (ft)	Elevation (ft)
1.	0.	0.
2.	20000.	0.

Leading vehicle speed table:

	Time (sec)	speed (mph)
1.	0	50.
2.	100	50.
3.	120	40.
4.	220	40.
5.	250	50.
6.	400	50.
7.	450	60.
8.	500	60.